VECTOR QUANTIZATION

WITH DIFFERENCE DISTORTION MEASURES

Yoshio Yamada

September, 1984

VECTOR QUANTIZATION
WITH DIFFERENCE DISTORTION MEASURES

（差歪測度のもとでのベクトル量子化に関する研究）

Yoshio Yamada

September, 1984

Abstract

This paper presents the performance of the vector quantization with the difference distortion measures.

In Chapter 1, the outline of this work is described after introducing the basic concept of the quantization.

In Chapter 2, the asymptotic bounds to the optimal performance of vector quantizers with finite block length are derived for the general distortion measures that are increasing functions of the seminorm of their argument, where any seminorm is allowed. When the distortion measure is a power of a seminorm the bounds are shown to be strictly better than the corresponding bounds provided by the k-th order rate distortion functions.

In Chapter 3, the asymptotic performance of variance-mismatched vector quantizers is investigated. It is demonstrated by both asymptotic analysis and computer simulations that well-designed vector quantizers are inherently more invulnerable to variance mismatch than conventional scalar quantizers.

In Chapter 4, the vector quantization is then applied to video signals. Based on the asymptotic analysis in Chapter 2, the vector quantization with maximum error distortion measure is discussed. Computer simulations are also performed to demonstrate the effectiveness of the vector quantization for real video signals.

In Chapter 5, the principal results of this work are summarized.

Acknowledgment

This work has been made at Tazaki Laboratory of Department of Electronics Engineering, Ehime University, and in part from May, 1980 to Feburary, 1981, at Namekawa Laboratory of Department of Communication Engineering, Osaka University.

I would like to express my heartfelt gratitude to Professor Toshihiko Namekawa of Department of Communication Engineering, Osaka University and Professor Saburo Tazaki of Department of Electronics Engineering, Ehime University for their continuous support and encouragement to this work.

I gratefully appreciate to Professor Nobuyuki Kumagai, Professor Yoshiroh Nakanishi, and Professor Yoshikazu Tezuka of Department of Communication Engineering, Osaka University, for their valuable criticisms and suggestions.

I owe a great deal to Associate Professor Masao Kasahara of Department of Communication Engineering, Osaka University, and Professor Robert M. Gray of Electrical Engineering, Stanford University. They made numerous informative discussions and suggestions during the years of this work.

I also appreciate to Associate Professor Hisashi Osawa of Department of Electronics Engineering, Ehime University, for his encouragement and helpful suggestions.

As a visiting researcher at Namekawa Laboratory, I benefited greatly from technical interaction with Assistant

Professor Tadashi Murata and Assistant Professor Masashi Sato, other staffs and graduate students.

My thanks also go to the students of Tazaki Laboratory for their cooperation and discussions.

Lastly but not least, thanks are due to the staffs of Department of Electronics Engineering, Ehime University for their encouragement and cooperation.

Table of Contents

List of Figures

List of Tables

Chapter 1

Introduction

1.1 Vector and Scalar Quantizations

Quantization is a deterministic mapping from an analog or continuous information source with infinite information contents (entropy) to a digital or discrete information source with finite information contents. By quantizing the analog source, we can produce the digital counterpart which approximately simulates the corresponding analog source. In other words, the approximated digital source can be encoded, transmitted over a digital channel, decoded, and reproduced at the destination yielding the quantized version of the original analog source. The goal of the quantization is the data compression which minimizes information rate while maintaining the necessary fidelity of such reproduction at the destination, or conversely, maximizes the fidelity of the reproduction within a given restriction on the information rate.

Because of their simplicity, the scalar quantizers have been used in the various signal processing and data compression systems [1]. For example, the Pulse Code Modulation (PCM) is the most common and well established digital communication technique [2]. However, from the information-theoretical point of view, the scalar quantizers provide rather poor performance for relatively low

information rate, approximately one bit per symbol (or sample) or less, whereas they provide good performance when large information rate is allowed [3].

The rate distortion theory shows us that the optimal analog-to-digital conversion can be achieved by quantizing a block of symbols at once instead of quantizing a individual source output symbol [4]. Such a block source coding or multi-dimensional quantization can provide optimal performance given by the rate distortion bound in the limit when the block length tends to infinity. It is these class of quantizers, which are referred to as the vector quantizers, that we investigate in the following Chapters.

1.2 Scope of This Work

Although the vector quantization technique is promised to success by the rate distortion theory, we have two problems to be solved so as to apply it with good success in practical communication systems, namely:

Problem 1. How good performance over the scalar quantizers can be achieved by the vector quantizers with finite block length?

Problem 2. How to construct or design the optimal or suboptimal vector quantizers?

This work is devoted to Problem 1.

In Chapter 2, the asymptotic bounds on the optimal performance of the vector quantizers are derived for the general difference distortion measures that are increasing

functions of the seminorm of the error vector. When the distortion measure is a power of a seminorm the bounds are shown to be strictly better than the corresponding bounds provided by the k-th order rate distortion functions.

In Chapter 3, the asymptotic bound on the optimal performance obtainable by the mismatched vector quantizers is derived for the distortion measures that are powers of a seminorm of the error vector. It is demonstrated by both asymptotic analysis and computer simulations that well-designed vector quantizers are inherently more invulnerable to the variance mismatch than conventional scalar quantizers.

In Chapter 4, the vector quantization is then applied to video signals. Based on the asymptotic analysis in Chapter 2, the vector quantization with the maximum error distortion measure is discussed under the mean-squared-error fidelity criterion. Computer simulations are also performed to demonstrate the effectiveness of the vector quantization for real video signals.

In Chapter 5, the principal results of this work are summarized.

Chapter 2

Asymptotic Performance of Vector Quantizers with Difference Distortion Measures [5]-[7]

2.1 Introduction

In a recent paper Gersho [8] provided a heuristic derivation of the tradeoffs between the rate and the average distortion for block or vector quantizers in the limit of large rate or small distortion. His work provides a unified and general development of many existing results for the asymptotic performance of scalar and block quantizers. In particular, he developed a k-dimensional analog to Bennett's [9] integral giving an approximation to the average distortion and used a simple technique of Gray and Gray [10] to obtain the performance of optimal quantizers (minimum average distortion) for a fixed rate. Gersho used as a vector distortion measure the r-th power of the Euclidean or the l_2 norm. To be precise, if a vector $\mathbf{x} \in \mathbf{R}^k$ is reproduced by a vector $\mathbf{y} \in \mathbf{R}^k$, then the resulting distortion is given by

$$d(\mathbf{x},\mathbf{y}) = \|\mathbf{x}-\mathbf{y}\|_2^r = \left\{ \sum_{j=1}^{k} |x_j-y_j|^2 \right\}^{r/2}$$

where $\|\cdot\|_2$ is a Euclidean or l_2 norm on $\mathbf{R}^k$. Gersho's approximation is a function of a "quantization coefficient" C(k,r) depending only on the dimension k and the power r. This coefficient is known only for the cases k = 1 and 2, and hence Gersho provides bounds to C(k,r) for general k. In

particular, he finds a lower bound to C(k,r) in terms of the known volume of a unit sphere in $\mathbf{R}^k$, and this provides general tractable lower bounds to the asymptotic distortion and the optimal trade-off between the average distortion and rate. It is these lower bounds that we generalize here.

In their classic paper on scalar quantizers (k = 1), Gish and Pierce [11] allowed more general difference distortion measures of the form

$$d(x,y) = L(x-y),$$

where L is a function such that

a) $L(0) = 0$,

b) $L(x)$ is an increasing function of x,

c) the function $M(v)$ defined by

$$M(v) = \frac{1}{2}\int_{-1}^{1} L(\alpha v/2)\, d\alpha \qquad (2.1)$$

is such that $vM'(v)$ is monotone for $v \geq 0$ (the prime denotes a derivative).

Gish and Pierce characterized the optimum trade-off between the average distortion and quantizer output entropy for this general distortion measure. For the special case of $L(x) = |x|^r$, the r-th power distortion, Algazi [12] characterized the trade-off between the average distortion and the quantizer alphabet size. Gray and Gray [10] made the slightly stronger assumption that $M(v)$ is convex $\cup$ and used Gish and Pierce's Bennett-style approximation for the asymptotic distortion to obtain a simple proof of the Gish-Pierce result via Hölder's and Jensen's inequalities instead of variational techniques. Gray and Gray [10] also provided

a similar simple proof for Algazi's result.

In this Chapter we combine Gersho's Euclidean norm approach with an adaptation of a technique of Yamada and Tazaki [13] for l_ν norms to obtain a k-dimensional generalization of the one-dimensional bounds of Gish and Pierce [11] and Algazi [12]. The distortion measures considered here have the general form $d(\mathbf{x},\mathbf{y}) = L(\mathbf{x}-\mathbf{y})$, where $L(\mathbf{0}) = 0$ and $L(\mathbf{u}) \leq L(\mathbf{x})$ if and only if $\|\mathbf{u}\| \leq \|\mathbf{x}\|$, where $\|\cdot\|$ is an arbitrary seminorm on $\mathbf{R}^k$. For some of the results a k-dimensional generalization of the Gish-Pierce function $M(v)$ of (2.1) is required to be convex. Our asymptotic bounds on distortion and on the optimal distortion-rate trade-off are natural generalizations of the bounds of Gersho, Gish-Pierce, and Algazi and take essentially the same form. For example, it is shown that for the general case considered uniform vector quantization asymptotically yields the minimum distortion quantizer subject to a quantizer output entropy constraint. The various bounds developed here are simplified for several specific special cases such as $d(\mathbf{x},\mathbf{y}) = \|\mathbf{x}-\mathbf{y}\|_\nu^r$, powers of the l_ν norms.

These asymptotic bounds are useful since they provide insight into the optimal distortion-rate trade-offs for vector quantizers with many output levels. For example, they provide an asymptotic reproduction vector distribution for quantizers minimizing the average distortion for a constrained number of reproduction vectors or a constrained quantizer output entropy. In addition, such performance bounds are often tighter than the general lower bounds provided by the rate-distortion theory [4] (as will be seen

in Section 2.5). Furthermore, it is often the case experimentally that these bounds are fairly accurate when the number of allowed reproduction vectors is only moderate [14].

Our development and notation parallel those of Gersho [8] and Gray and Gray [10] to ease the comparison of assumptions and results.

2.2 Preliminaries

2.2.1 Vector Quantization and Distortion Measures

Let $\mathbf{X}$ be a k-dimensional random vector taking sample values $\mathbf{x}$ as described by a joint probability density function $p(\mathbf{x})$, where $\mathbf{x} = (x_1, x_2, \ldots, x_k) \in \mathbf{R}^k$, k-dimensional Euclidean space. A k-dimensional (or block or vector) quantizer Q is described by a collection of N reproduction vectors $y_1, y_2, \ldots, y_N \in \mathbf{R}^k$, called the reproduction alphabet or quantizer output alphabet, and a partition $\{ S_1, S_2, \ldots, S_N \}$ of $\mathbf{R}^k$ (the atoms S_i are disjoint and exhaust $\mathbf{R}^k$). The quantizer Q is defined by

$$Q(\mathbf{x}) = \mathbf{y}_i, \quad \text{if } \mathbf{x} \in S_i.$$

Let $\| \mathbf{x} \|$ be a seminorm on $\mathbf{R}^k$, that is,

$$\| \mathbf{x} \| \geq 0,$$

$$\| a\mathbf{x} \| = |a| \cdot \| \mathbf{x} \| \qquad \text{for all } a \in \mathbf{R}^1,$$

and

$$\| \mathbf{x}+\mathbf{y} \| \leq \| \mathbf{x} \| + \| \mathbf{y} \|.$$

Common examples are l_ν or Hölder norms defined by

$$\|\mathbf{x}\|_\nu = \left\{ \sum_{j=1}^{k} |x_j|^\nu \right\}^{1/\nu},$$

which for $\nu = 2$ is the usual Euclidean norm, the supremum or l_∞ norm,

$$\|\mathbf{x}\|_\infty = \lim_{\nu\to\infty} \|\mathbf{x}\|_\nu = \sup_j |x_j|,$$

and the inner product or quadratic norms of the form

$$\|\mathbf{x}\|^2 = (\mathbf{x},\mathbf{x}),$$

where $(\cdot,\cdot)$ is an inner product on $\mathbf{R}^k$. An example of an inner product norm is

$$\|\mathbf{x}\| = \left\{ \mathbf{x}\mathbf{B}\mathbf{x}^t \right\}^{1/2} = \left\{ \sum_{i=1}^{k} \sum_{j=1}^{k} x_i x_j B_{ij} \right\}^{1/2}$$

where t denotes transpose and **B** is a k x k symmetric nonnegative definite matrix.

The distortion resulting from reproducing a vector **x** as **y** is defined as a difference distortion measure by

$$d(\mathbf{x},\mathbf{y}) = L(\mathbf{x}-\mathbf{y}), \tag{2.2}$$

where

a) $L(\mathbf{0}) = 0$ (2.3)

b) $L(\mathbf{u}) < L(\mathbf{x})$ if and only if $\|\mathbf{u}\| \leq \|\mathbf{x}\|$, (2.4)

that is, L is an increasing function of the seminorm of its argument. These are exactly the k-dimensional counterparts of the assumptions a) and b) of Gish and Pierce [11] and Gray and Gray [10] where k = 1 and $\|\mathbf{x}\| = |x|$, the absolute value. Unlike Gersho [8], we do not normalize d by 1/k and this clutters the initial development.

Given a set $G \subset R^k$, define its volume V(G) by

$$V(G) = \int_G d\mathbf{x}.$$

This is simply the Lebesgue measure of G in R^k --- we assume that G is a Borel set so that V(G) is defined. In particular, we define the volume of the unit sphere in k-dimensional space by

$$V_k = V(\{\mathbf{u}: \|\mathbf{u}\| \leq 1\}). \tag{2.5}$$

We assume that $V_k < \infty$. For example, from Gradshteyn and Ryzhik [15,p.620] for l_ν norms

$$V_k = V_k(\nu) = \frac{2^k(\Gamma(1/\nu))^k}{k\Gamma(k/\nu)\nu^{k-1}} . \tag{2.6a}$$

For the l_∞ norm

$$V_k = V_k(\infty) = \int_{\mathbf{u}:u_i\varepsilon[0,1],i=1,2,\ldots,k} d\mathbf{u} = 1, \tag{2.6b}$$

that is, here V_k is the "unit cube" in R^k. For the quadratic norm $\|\mathbf{x}\|^2 = \mathbf{x}\mathbf{B}\mathbf{x}^t$ from standard matrix theory and a linear change of variables,

$$\begin{aligned} V_k &= \{\det\mathbf{B}\}^{-1/2}V_k(2) \\ &= \{\det\mathbf{B}\}^{-1/2} \frac{2\Gamma(1/2)^k}{k\Gamma(k/2)} , \end{aligned} \tag{2.6c}$$

where $\Gamma(1/2) = \sqrt{\pi}$. Our bounds will depend on V_k, which is computable for most interesting norms.

Observe also that the volume of a sphere of radius a centered at $\mathbf{y}$ is given by

$$V_k = V(\{\mathbf{x} : \|\mathbf{x}-\mathbf{y}\| \leq a\}) = V(\{\mathbf{x} : \|\mathbf{x}\| \leq a\})$$

$$= \int_{\mathbf{x} : \|\mathbf{x}\| \leq a} d\mathbf{x}$$

$$= \int_{\mathbf{x} : \|\mathbf{x}/a\| \leq 1} d\mathbf{x}$$

$$= \int_{\mathbf{u} : \|\mathbf{u}\| \leq 1} a^k d\mathbf{u}$$

$$= a^k V_k, \qquad (2.7)$$

since volume is invariant to translation.

2.2.2 Generalization of Gish-Pierce Function

The appropriate generalization of the Gish-Pierce function $M(v)$ to the case considered is given by

$$M_k(v) = \frac{1}{V_k} \int_{\mathbf{u} : \|\mathbf{u}\| \leq 1} L(V_k^{-1/k} v\,\mathbf{u})\, d\mathbf{u}$$

$$= v^{-k} \int_{\mathbf{x} : \|\mathbf{x}\| \leq v V_k^{-1/k}} L(\mathbf{x})\, d\mathbf{x}. \qquad (2.8)$$

This form of $M_k(v)$ is chosen for mathematical convenience. By way of interpretation, however, observe that if we define the sphere $F = \{\mathbf{x}: \|\mathbf{x}\| \leq v V_k^{-1/k}\}$, where the $V_k^{-1/k}$ can be viewed as a fixed scaling of the radius variable v, then

$$V_k M_k(v) = \left\{ V_k^{1/k}/v \right\}^k \int_F L(\mathbf{x})\, d\mathbf{x}$$

$$= \frac{1}{V(F)} \int_F L(\mathbf{x})\, d\mathbf{x}.$$

The latter integral is the average distortion resulting if a

random vector uniformly distributed on F is represented by a single reproduction vector **0** at the center of the sphere F. Thus , for fixed k, $M_k(v)$ is a suitably scaled measure of the average distortion resulting when a random vector uniformly distributed on a sphere of radius proportional to v is reproduced as the center of the sphere.

For k = 1 and $\|\mathbf{u}\| = |u|$, $V_1 = 2$ and hence $M_1(v)$ reduces to $M(v)$ of (2.1). We shall later require that

c) $M_k(v)$ is convex U,

the k-dimensional analog of the assumption in [10]. We next consider some important special cases.

In some cases the function L depends on its argument only through the norm of the argument. This is analogous to the one-dimensional case where $L(\alpha) = L(|\alpha|)$, that is, L is symmetric or depends on its argument only through its magnitude. If $\|\mathbf{u}\| = \|\mathbf{x}\|$ implies $L(\mathbf{u}) = L(\mathbf{x})$, then there is a function $\rho:[0,\infty) \to [0,\infty)$ such that $L(\mathbf{u}) = \rho(\|\mathbf{u}\|)$ and the distortion takes the form

$$d(\mathbf{x},\mathbf{y}) = \rho(\|\mathbf{x}-\mathbf{y}\|),$$

where $\rho(0) = 0$ and $\rho(\alpha)$ is increasing with α. We will call such a distortion measure a norm based distortion measure.

The integral of (2.8) can be simplified in the case of a norm-based distortion measure as follows. We can rewrite (2.8) as

$$M_k(v) = \int_{\mathbf{u}:\|\mathbf{u}\| \leq 1} \rho(V_k^{-1/k} v \|\mathbf{u}\|) dm(\mathbf{u}) \qquad (2.9)$$

where m is the Lebesgue measure on $\mathbf{R}^k$ (see, for example, Rudin [16,p.50]). Given any integral of the form

$$\int_{\|u\|\in G} f(\|u\|)\,dm(u),$$

where $f:R^1 \to R^1$ is measurable and $G \subset R^1$ is a Borel set, since the mapping $T:R^k \to R^1$ defined by $T(u) = \|u\|$ is continuous and hence measurable, we can change variables as in Ash [17,p.50] to write the above integral as

$$\int_{u\in T^{-1}G} f(T(u))\,dm(u) = \int_{\beta\in G} f(\beta)\,dmT^{-1}(\beta)$$

The measure $mT^{-1}(\beta)$ is a Lebesgue-Stieltjes measure on R^1; hence the above integral can be written using a distribution function (e.g., Ash [17,sec.1.4]) as

$$\int_{\beta\in G} f(\beta)\,dF(\beta)$$

where

$$F(\beta) = mT^{-1}((-\infty,\beta)) = m(u:\|u\| \leq \beta) = \beta^k V_k$$

yielding

$$\int_{\|u\|\in G} f(\|u\|)\,dm(u)$$

$$= V_k \int_{\beta\in G} f(\beta)\,d(\beta^k)$$

$$= V_k \int_{\alpha^{1/k}\in G} f(\alpha^{1/k})\,d\alpha$$

$$= kV_k \int_{\beta\in G} f(\beta)\beta^{k-1}d\beta \qquad (2.10)$$

where the only dependence on the particular norm chosen is through V_k. Using (2.10) to evaluate (2.9) yields

$$M_k(v) = \int_0^1 \rho(v\{\alpha/V_k\}^{1/k})\,d\alpha$$

$$= k \int_0^1 \rho(vV_k^{-1/k}\beta)\beta^{k-1}d\beta \qquad (2.11)$$

In the further special case of a norm-based distortion measure with $\rho(\alpha) = \alpha^r$, $r \geq 1$, (2.11) becomes

$$M_k(v) = v^r V_k^{-r/k} \int_0^1 \alpha^{r/k} d\alpha$$
$$= \frac{k v^r}{k+r} V_k^{-r/k}, \qquad (2.12)$$

which is indeed convex U.

Note that in the above special cases $M_k(v)$ depends on the actual norm chosen only though the volume V_k of the unit sphere. Observe also that the special case $d(\mathbf{x},\mathbf{y}) = \|\mathbf{x}-\mathbf{y}\|_r^r$ allows one to place an r-th low distortion on the individual symbols (unlike Gersho's distortion $\|\mathbf{x}-\mathbf{y}\|_2^r$).

2.2.3 Average Distortion and Rate

The performance of a quantizer Q is measured by the average distortion

$$D = E\{d(\mathbf{X},Q(\mathbf{X}))\}$$
$$= E\{L(\mathbf{X}-Q(\mathbf{X}))\}$$
$$= \int d\mathbf{x}\, p(\mathbf{x})\, L(\mathbf{x}-Q(\mathbf{x}))$$
$$= \sum_{i=1}^{N} \int_{S_i} d\mathbf{x}\, p(\mathbf{x})\, L(\mathbf{x}-\mathbf{y}_i) \qquad (2.13)$$

We assume that $E\{L(\mathbf{X})\} < \infty$. The rate of a quantizer Q is measured either by the quantizer output entropy H_Q defined by

$$H_Q = -\sum_{i=1}^{N} p_i \log p_i,$$
$$p_i = \int_{S_i} p(\mathbf{x})\, d\mathbf{x} = \Pr(\mathbf{x} \varepsilon S_i), \qquad (2.14)$$

or by log N (logarithms are base e).

2.3 Asymptotic Distortion

2.3.1 Assumptions for Asymptotic Analysis

In this section we obtain a lower bound to the asymptotic average distortion D for the distortion measures $d(\mathbf{x},\mathbf{y})$ of (2.2) satisfying properties a) and b).

The initial fundamental assumption in all studies of asymptotic quantization is that the probability density $p(\mathbf{x})$ is sufficiently "smooth" to ensure that $p(\mathbf{x})$ is effectively constant over small bounded atoms. In particular, for N large enough we have for all bounded atoms (decision regions) $p(\mathbf{x}) \cong b_i$ for $\mathbf{x} \in S_i$, and hence from (2.14)

$$p_i = \int_{S_i} p(\mathbf{x})\, d\mathbf{x} \cong b_i \int_{S_i} d\mathbf{x} = b_i V(S_i)$$

or

$$p(\mathbf{x}) \cong p_i/V(S_i), \quad \mathbf{x} \in S_i. \tag{2.15}$$

Assume as in Gersho that for N large most of the atoms S_i will be bounded and the "overload" region will correspond to the tail region of the density $p(\mathbf{x})$. Assuming that the partition is appropriately chosen so that the overload region is negligible, taking N as the number of bounded atoms (this is possible since $E\{L(\mathbf{X})\} < \infty$), and then combining (2.15) and (2.13) yields

$$D = \sum_{i=1}^{N} (p_i/V(S_i)) \int_{S_i} d\mathbf{x}\, L(\mathbf{x}-\mathbf{y}_i). \tag{2.16}$$

2.3.2 Effective Radius and Effective Region

For a bounded set $S \varepsilon R^k$, we define the effective radius $R(S)$ of S by

$$R(S) = \{V(S)/V_k\}^{1/k} \tag{2.17}$$

where

$$V_k = V(\{\mathbf{u}: \|\mathbf{u}\| \leq 1\}).$$

From (2.7) $R(S)$ is the radius of a sphere having the same volume as S. Fix $S \subset R^k$ and $\mathbf{y} \varepsilon R^k$ and define the effective region $T(S)$ of S centered at $\mathbf{y}$ by

$$T(S) = \{\mathbf{x}: d(\mathbf{x},\mathbf{y}) \leq L(R(S)\cdot\mathbf{e})\} \tag{2.18a}$$

where $\mathbf{e} \varepsilon R^k$ is any vector with the unit norm ($\|\mathbf{e}\| = 1$). From (2.4)

$$d(\mathbf{x},\mathbf{y}) = L(\mathbf{x}-\mathbf{y}) \leq L(R(S)\cdot\mathbf{e})$$

if and only if

$$\|\mathbf{x}-\mathbf{y}\| \leq R(S)\cdot\|\mathbf{e}\| = R(S)$$

and therefore,

$$T(S) = \{\mathbf{x}: \|\mathbf{x}-\mathbf{y}\| \leq R(S)\}. \tag{2.18b}$$

That is, $T(S)$ is a sphere of radius $R(S)$ about $\mathbf{y}$, and hence from (2.7)

$$V(T(S)) = R(S)^k V_k = V(S). \tag{19}$$

Fix $S \subset R^k$ and let $G = S \cup T(S)$. We then have

$$S \cup (G-S) = T(S) \cup (G-T(S)) = G$$

(where $G-S = G \cap S^c$),

$$\int_G d(\mathbf{x}-\mathbf{y})\,d\mathbf{x} = \int_S d(\mathbf{x},\mathbf{y})\,d\mathbf{x} + \int_{G-S} d(\mathbf{x},\mathbf{y})\,d\mathbf{x}$$

$$= \int_{T(S)} d(\mathbf{x},\mathbf{y})\,d\mathbf{x} + \int_{G-T(S)} d(\mathbf{x},\mathbf{y})\,d\mathbf{x},$$

and, therefore,

$$\int_S d(\mathbf{x},\mathbf{y})\,d\mathbf{x}$$

$$= \int_{T(S)} d(\mathbf{x},\mathbf{y})\,d\mathbf{x} + \int_{G-T(S)} d(\mathbf{x},\mathbf{y})\,d\mathbf{x} - \int_{G-S} d(\mathbf{x},\mathbf{y})\,d\mathbf{x}. \qquad (2.20)$$

2.3.3 Lower Bounds

From (2.18) and (2.19), (2.20) yields the lower bound

$$\int_S d(\mathbf{x},\mathbf{y})\,d\mathbf{x}$$

$$\geq \int_{T(S)} d(\mathbf{x},\mathbf{y})\,d\mathbf{x} + \int_{G-T(S)} L(R(S)\mathbf{e})\,d\mathbf{x} - \int_{G-S} L(R(S)\mathbf{e})\,d\mathbf{x}.$$

$$= \int_{T(S)} d(\mathbf{x},\mathbf{u})\,d\mathbf{x} + L(R(S)\mathbf{e})\{V(G-T(S))-V(G-S)\}$$

$$= \int_{T(S)} d(\mathbf{x},\mathbf{y})\,d\mathbf{x} + L(R(S)\mathbf{e})\{V(G)-V(T(S))-V(G)+V(S)\}$$

$$= \int_{T(S)} d(\mathbf{x},\mathbf{y})\,d\mathbf{x} \qquad (2.21)$$

This is a generalized version of Gersho's observation that a convex polytope has a greater moment of inertia with respect to its centroid than does a k-dimensional sphere with the same volume. Here, however, S need not be a polytope nor convex and the sphere can be defined via any seminorm on R^k. Equality will hold in (2.21) if and only if T(S) = S, that is, S is a sphere.

Next observe that

$$\int_{T(S)} d(\mathbf{x},\mathbf{y})\,d\mathbf{x}$$

$$= \int_{\mathbf{x}:\,\|\mathbf{x}-\mathbf{y}\| \le R(S)} L(\mathbf{x}-\mathbf{y})\,d\mathbf{x}$$

$$= \int_{\mathbf{x}:\,\|\mathbf{x}\| \le R(S)} L(\mathbf{x})\,d\mathbf{x}$$

$$= \int_{\mathbf{x}:\,\|\mathbf{x}/R(S)\| \le 1} L(\mathbf{x})\,d\mathbf{x}$$

$$= R(S)^k \int_{\mathbf{u}:\,\|\mathbf{u}\| \le 1} L(R(S)\mathbf{u})\,d\mathbf{u} \qquad (2.22)$$

where $\mathbf{u} = \mathbf{x}/R(S)$. Thus from (2.17),(2.21),(2.22), and (2.8)

$$\int_S d(\mathbf{x},\mathbf{y})\,d\mathbf{x} \ge \frac{V(S)}{V_k} \int_{\mathbf{u}:\,\|\mathbf{u}\| \le 1} L((V(S)/V_k)^{1/k}\mathbf{u})\,d\mathbf{u}$$

$$= V(S)\; M_k(V(S)^{1/k}) \qquad (2.23)$$

Applying (2.23) to S_i, $\mathbf{y}_i$, i=1,2,...,N, and using (2.16) yields the asymptotic (large N) lower bound

$$D \ge \sum_{i=1}^{N} p_i\, M_k(V(S_i)^{1/k}). \qquad (2.24)$$

Following Gersho [8], define the k-dimensional reproduction vector density by

$$g_N(\mathbf{x}) = (NV(S_i))^{-1} \text{ if } \mathbf{x}\varepsilon S_i,\ i=1,2,\ldots,N,$$

and assume that as $N \to \infty$ there is a limiting density $\lambda(\mathbf{x})$ having unit integral and hence

$$V(S_i) \cong (N\lambda(\mathbf{y}_i))^{-1} \qquad (2.25)$$

for every bounded atom S_i. In other words, $\lambda(\mathbf{x})\cdot\Delta V(\mathbf{x})$ is the fraction of reproduction vectors in an incremental volume containing $\mathbf{x}$. Using this approximation in (2.24) yields

$$D \geq \sum_{i=1}^{N} p_i \, M_k((N\lambda(y_i))^{-1/k}) \tag{2.26}$$

which we approximate by

$$D \geq \int dy p(y) M_k((N\lambda(y))^{-1/k})$$

$$= E\{M_k((N\lambda(X))^{-1/k})\} \triangleq D_L. \tag{2.27}$$

As an example, if $L(x) = \|x\|^r$, then from (2.12)

$$D \geq \frac{k}{k+r} \{NV_k\}^{-r/k} E\{\lambda(X)^{-r/k}\}, \tag{2.28}$$

which generalizes Gersho's lower bound [8,eq.(18) and (10)] from an l_2 norm to any seminorm. The only difference is the actual value of V_k.

For the case of k = 1, (2.27) is known to hold with equality as $N \to \infty$ and is a form of Gish and Pierce [11,eq.(16)]. This is true since in one dimension the atoms S_i become spheres (intervals) as $N \to \infty$ and hence in (2.23)-(2.27) they become asymptotic equalities. In higher dimensions one generally cannot partition the space with spheres and only the bound results. For the case $L(x-y) = \|x-y\|_2^r$ Gersho [8] provides a heuristic development of a similar expression to (2.27) which provides an actual approximation to D which is then used to obtain the bound (2.27). Gersho's approximation is obtained by using non-spherical effective regions, that is, replacing T(S) by convex polytopes that actually approximate S for large N. His approach can be adapted to the special case $L(x) = \|x\|^r$, but it seems to be of limited use when norms other

than ℓ_2 norms are used since his coefficient of quantization cannot be evaluated in general. Hence we confine ourselves to the lower bounds. We shall later provide an example of the asymptotic difference between the bound and the approximation in the case k = 2 where the approximation can be evaluated.

2.4 Bounds on Asymptotic Optimal Performance

2.4.1 Bound for Entropy Rate

We now assume that the distortion measure also satisfies the condition c). As in Gersho [8], combining (2.14) with its approximations (2.15) and (2.25) yields

$$H_Q \cong h(p) - E\left\{\log\left[\frac{1}{N\lambda(\mathbf{X})}\right]\right\} \tag{2.29}$$

where

$$h(p) = -\int d\mathbf{x}\; p(\mathbf{x})\; \log\; p(\mathbf{x}) \tag{2.30}$$

is the differential entropy. Using Jensen's inequality we find

$$\begin{aligned} H_Q &\cong h(p) - k\, E\left\{\log\left[\frac{1}{N\lambda(\mathbf{X})}\right]^{1/k}\right\} \\ &\geq h(p) - k \log E\left\{\left[\frac{1}{N\lambda(\mathbf{X})}\right]^{1/k}\right\}. \end{aligned} \tag{2.31}$$

Since M_k is assumed to be convex, application of Jensen's inequality to (2.27) yields

$$D \geq D_L \geq M_k\left[E\left\{\left[\frac{1}{N\lambda(\mathbf{X})}\right]^{1/k}\right\}\right] \tag{2.32}$$

or

$$M_k^{-1}(D) \geq M_k^{-1}(D_L) \geq E\left\{\left(\frac{1}{N\lambda(\mathbf{X})}\right)^{1/k}\right\}, \qquad (2.33)$$

where the inverse is well-defined since M_k is convex. Combining (2.31) and (2.33) yields

$$\begin{aligned} H_Q &\geq h(p) - k \cdot \log M_k^{-1}(D_L) \\ &\geq h(p) - k \cdot \log M_k^{-1}(D) \end{aligned} \qquad (2.34)$$

which provides a lower bound to the asymptotically achievable quantizer output entropy for fixed D. Assuming natural logarithms we can rewrite (2.34) as

$$\exp\left[-(H_Q - h(p))/k\right] \leq M_k^{-1}(D_L) \leq M_k^{-1}(D), \qquad (2.35)$$

so

$$D \geq D_L \geq M_k\left[\exp\left[-(H_Q - h(p))/k\right]\right], \qquad (2.36)$$

which provides a lower bound to the asymptotically achievable average distortion for fixed quantizer entropy.

For k = 1, (2.34) reduces to [10,eq.(7)]. When $L(\mathbf{x}) = \|\mathbf{x}\|^r$, (2.36) becomes

$$D \geq D_L \geq \frac{k V_k^{-r/k}}{k + r} \exp\left[-(r/k)(H_Q - h(p))\right] \qquad (2.37)$$

which generalizes the bound of [8,eq.(23) and (10)] to arbitrary seminorms.

In the above applications of Jensen's inequality, equality holds in the right-hand inequalities of (2.32), (2.36), and (2.37) if and only if $\lambda(\mathbf{x})$ is constant on a set G such that

$$\int d\mathbf{x}\, p(\mathbf{x}) = 1.$$

Since λ has a unit integral, G must be bounded. Thus D_L equals its lower bound if and only if all the source measure is on a bounded set and $\lambda(\mathbf{x})$ is uniform on that set. If $p(\mathbf{x})$ has well-behaved tails, then approximate equality can be achieved if $\lambda(\mathbf{x})$ is constant on a set G such that

$$\Pr(\mathbf{x} \varepsilon G) \cong 1.$$

2.4.2 Bound for Codebook Rate

Next consider the case where the rate is measured by log N. As in [10] we consider only the case $L(\mathbf{x}) = \|\mathbf{x}\|^r$. Apply Hölder's inequality to (2.28) exactly as in [10,eq.(8)] with k-dimensional integrals or as in [8,sec.VI] to obtain

$$D \geq D_L = \frac{k}{k+r} (V_k N)^{-r/k} E\left\{ \lambda(\mathbf{X})^{-r/k} \right\}$$

$$\geq \frac{k}{k+r} (V_k N)^{-r/k} \|p\|_{k/(k+r)} \qquad (2.38)$$

where here the norm denotes the $L_{k/(k+r)}$ norm on real functions defined on R^k. The right-hand inequality in (2.38) is an equality if and only if $\lambda(\mathbf{x})$ is proportional to $p(\mathbf{x})^{k/(k+r)}$. This generalizes Gersho's bound [8,eq.(19) and (10)] to arbitrary seminorms. Again the only difference is the value of V_k. Note in particular that the condition for equality is independent of the particular norm chosen.

2.4.3 Examples

Denote the k-dimensional probability $p(\mathbf{x})$ by p_k and define the per-symbol differential entropy $h_k = k^{-1}h(p_k)$ and per-symbol quantizer output entropy $H_k = H_Q/k$. We specialize the previous results to several examples of norm-based distortion measures.

For an arbitrary norm we have from (2.36) and (2.11) that

$d(\mathbf{x},\mathbf{y}) = \rho(\|\mathbf{x}-\mathbf{y}\|)$:

$$D \geq D_L \geq k \int_0^1 \rho\left(\exp(-(H_k-h_k))V_k^{-1/k}\beta\right)\beta^{k-1}d\beta. \quad (2.39)$$

$d(\mathbf{x},\mathbf{y}) = \rho(\|\mathbf{x}-\mathbf{y}\|_\nu)$:

For l_ν norms we have from (2.6) that

$D \geq D_L \geq$

$$\geq k \int_0^1 \rho\left(\exp(-(H_k-h_k))\left(\frac{k\Gamma(k/\nu)}{\nu}\right)^{1/k}\left(\frac{\nu}{2\Gamma(1/\nu)}\right)\beta\right)\beta^{k-1}d\beta. \quad (2.40)$$

$d(\mathbf{x},\mathbf{y}) = \rho(\|\mathbf{x}-\mathbf{y}\|_\infty)$:

$$D \geq D_L \geq k \int_0^1 \rho\left(\exp(-(H_k-h_k))\ \beta\right)\beta^{k-1}d\beta. \quad (2.41)$$

$d(\mathbf{x},\mathbf{y}) = \rho(\{(\mathbf{x}-\mathbf{y})\mathbf{B}(\mathbf{x}-\mathbf{y})^t\}^{1/2})$:

$D \geq D_L \geq$

$$\geq k \int_0^1 \rho\left(\exp(-(H_k-h_k))\left(\frac{k\Gamma(k/2)(\det\mathbf{B})^{1/2}}{2}\right)^{1/k} \cdot \sqrt{\pi}\ \beta\right)\beta^{k-1}d\beta. \quad (2.42)$$

We next use (2.37),(2.38), and (2.6) to further specialize these results to the case $\rho(\alpha) = \alpha^r$, $r \geq 1$.

$d(\mathbf{x},\mathbf{y}) = \|\mathbf{x}-\mathbf{y}\|_\nu^r$:

$$D \geq D_L \geq \frac{k}{k+r}\left(\frac{\nu}{2\Gamma(1/\nu)}\right)^r \cdot \left(\frac{k\Gamma(k/\nu)}{\nu}\right)^{r/k} \exp(-r(H_k-h_k)), \tag{2.43}$$

$$D \geq D_L \geq N^{-r/k}\cdot\frac{k}{k+r}\left(\frac{\nu}{2\Gamma(1/\nu)}\right)^r \cdot \left(\frac{k\Gamma(k/\nu)}{\nu}\right)^{r/k} \|p_k\|_{k/(k+r)}\cdot \tag{2.44}$$

$d(\mathbf{x},\mathbf{y}) = \|\mathbf{x}-\mathbf{y}\|_\infty^r$:

$$D \geq D_L \geq \frac{k}{k+r}\exp(-r(H_k-h_k)), \tag{2.45}$$

$$D \geq D_L \geq N^{-r/k}\frac{k}{k+r}\|p_k\|_{k/(k+r)}\cdot \tag{2.46}$$

$d(\mathbf{x},\mathbf{y}) = \{(\mathbf{x}-\mathbf{y})\mathbf{B}(\mathbf{x}-\mathbf{y})^t\}^{r/2}$:

$$D \geq D_L \geq \frac{k\pi^{-r/2}}{k+r}\left\{\frac{k\Gamma(k/2)(\det\mathbf{B})^{1/2}}{2}\right\}^{r/k} \cdot \exp(-r(H_k-h_k)), \tag{2.47}$$

$$D \geq D_L \geq N^{-r/k}\cdot\frac{k\pi^{-r/2}}{k+r}\left\{\frac{k\Gamma(k/2)(\det\mathbf{B})^{1/2}}{2}\right\}^{r/k} \cdot \|p_k\|_{k/(k+r)}\cdot \tag{2.48}$$

Equality holds on the right in (2.39)-(2.43),(2.45), and (2.47) if and only if $\lambda(\mathbf{x}) = 1/V(G)$ on a bounded set G

of probability one. Equality holds on the right of (2.44),(2.46), and (2.48) if and only if $\lambda(\mathbf{x})$ is proportional to $p(\mathbf{x})^{k/(k+r)}$. Equality holds on the left in (2.39)-(2.48) if and only if the decision regions are approximately spheres in the given norm. This is possible, for example, in (2.41), (2.45) and (2.46) since the unit spheres are unit cubes which tessellate $\mathbf{R}^k$. This is not possible in general, although it may be approximately true in some cases.

We can also write these examples as follows. Let $\overline{R} = k^{-1}\log N$ denote the per-symbol codebook rate of the quantizer.

$d(\mathbf{x},\mathbf{y}) = \|\mathbf{x}-\mathbf{y}\|_\nu^r$:

$$H_k \geq h_k - r^{-1}\log D + r^{-1}\log(k/(k+r)) + \log\left\{\left(\frac{\nu}{2\Gamma(1/\nu)}\right)\left(\frac{k\Gamma(k/\nu)}{\nu}\right)^{1/k}\right\}, \qquad (2.49)$$

$$\overline{R} \geq \log\|p_k\|_{k/(k+r)}^{1/r} - r^{-1}\log D + r^{-1}\log(k/(k+r)) + \log\left\{\left(\frac{\nu}{2\Gamma(1/\nu)}\right)\left(\frac{k\Gamma(k/\nu)}{\nu}\right)^{1/k}\right\}. \qquad (2.50)$$

2.5 Comparison with Rate Distortion Theory

2.5.1 k-th Order Rate Distortion Function

Consider now distortion measures of the form $d(\mathbf{x},\mathbf{y}) = \|\mathbf{x}-\mathbf{y}\|^r$ where the seminorm is arbitrary. An alternative lower bound to the rate of a k-dimensional quantizer yielding expected distortion D is given by the k-th order rate distortion function $R^{(k)}(D)$ defined by

$$R^{(k)}(D) = \inf I(\mathbf{X},\mathbf{Y})$$

where the infimum is over all conditional densities $p(\mathbf{y}|\mathbf{x})$ yielding $E\{d(\mathbf{X},\mathbf{Y})\} < D$. For difference distortion measures the rate distortion function is further bounded by the Shannon lower bound $R_{SLB}^{(k)}(D)$ defined (if it exists) by

$$R_{SLB}^{(k)}(D) = h(p_k) + \log a(D) - Db(D)$$

where $a(D)$ and $b(D)$ are the solution of

$$a(D) \int_{R^k} \exp\left[-b(D)L(\mathbf{x})\right] d\mathbf{x} = 1.$$

$$a(D) \int_{R^k} L(\mathbf{x}) \exp\left[-b(D)L(\mathbf{x})\right] d\mathbf{x} = D.$$

This is the k-dimensional version of Berger [4, sec.4.3.1]. Furthermore, Lin'kov [18] shows that for sufficiently "nice" densities, $R^{(k)}(D) \cong R_{SLB}^{(k)}(D)$ as $D \to 0$. Hence $R_{SLB}^{(k)}(D)$ and the previous results both provide lower bounds to the performance of k-dimensional quantizers for D small, and it is of interest to compare these bounds both for k fixed and as $k \to \infty$.

First observe that we can use (2.10) to rewrite the above condition where $L(\mathbf{x}) = \rho(\|\mathbf{x}\|)$ in one-dimensional form as

$$1 = a(D)\, kV_k \int_0^\infty \exp\left[-b(D)\rho(\beta)\right] \beta^{k-1} d\beta,$$

$$D = a(D)\, kV_k \int_0^\infty \rho(\beta) \exp\left[-b(D)\rho(\beta)\right] \beta^{k-1} d\beta.$$

For the case $\rho(\beta) = \beta^r$ we have from [15,p.317] that

$$1 = a(D)\ kV_k \int_0^\infty \exp\left(-b(D)\beta^r\right)\beta^{k-1}d\beta$$

$$= a(D)\ kV_k \int_0^\infty \exp\left(-b(D)\alpha\right)\frac{\alpha^{(k/r)-1}}{r}\,d\alpha$$

$$= a(D)\ \frac{k}{r}\ V_k\ \frac{\Gamma(k/r)}{b(D)^{k/r}}\ ,$$

and similarly

$$D = a(D)\ kV_k \int_0^\infty \exp\left(-b(D)\alpha\right)\frac{\alpha^{k/r}}{r}\,d\alpha$$

$$= a(D)\ \frac{k}{r}\ V_k\ \frac{\Gamma((k/r)+1)}{b(D)^{(k/r)+1}}\ ,$$

yielding

$$a(D) = \frac{r}{kV_k}\ \frac{b(D)^{k/r}}{\Gamma(k/r)}$$

$$b(D) = \frac{\Gamma((k/r)+1)}{\Gamma(k/r)}\ \frac{1}{D} = \frac{k}{rD}\ ,$$

whence

$$R_{SLB}^{(k)}(D) = h(p_k) - \frac{k}{r} + \log\left\{\frac{r}{kV_k}\left(\frac{k}{rD}\right)^{k/r}\frac{1}{\Gamma(k/r)}\right\}$$

or normalizing rate to nats per dimension

$$\overline{R}_{SLB}^{(k)}(D) = k^{-1}\ R_{SLB}^{(k)}(D)$$

$$= h_k - \frac{1}{r}\log(D/k) - \frac{1}{k}\log V_k$$

$$- \frac{1}{r}\log\left\{er\Gamma(1+k/r)^{r/k}\right\}\ . \qquad (2.51)$$

For example, for l_ν norms we have from the above and (2.6a) that

$$\bar{R}_{SLB}^{(k)}(D) = h_k - \frac{1}{r}\log(D/k)$$

$$- \frac{1}{r}\log\left\{ er\left[\frac{2\Gamma(1/\nu)}{\nu}\right]^r\left[\frac{\Gamma(k/r)\nu}{k\Gamma(k/\nu)}\right]^{r/k}\right\} . \qquad (2.52)$$

We observe that the above development points out that Lin'kov's corollary 2 [18] is valid for the distortion measure $\|\mathbf{x}-\mathbf{y}\|_\alpha^{\alpha\beta}$ and not $n^{-\beta}\|\mathbf{x}-\mathbf{y}\|_\alpha^{\alpha\beta}$ as claimed (this can also be verified by direct substitution into Lin'kov's Theorem 1). Equation (2.51) provides the most general evaluation of the Shannon lower bound known to the author, and it is interesting that again the only dependence on the particular seminorm chosen is through V_k. As an alternative expression, let $D_{SLB}^{(k)}(R)$ denote the Shannon lower bound to the distortion-rate function. Rewriting (2.51) then yields

$$\bar{D}_{SLB}^{(k)}(R)$$

$$= k^{-1} D_{SLB}^{(k)}(R)$$

$$= \left\{ er\left[V_k\Gamma(1+k/r)\right]^{r/k}\right\}^{-1}\exp(-r(\bar{R}-h_k)) \qquad (2.53)$$

where $\bar{R} = R/k$.

2.5.2 Comparison

To compare the lower bounds of (2.51) and (2.53) with those previously developed we define the code book rate per dimension of a quantizer by $\bar{R} = k^{-1}\log N$ and observe that since $k^{-1}H_Q = H_k \leq \bar{R}$ we have from (2.37) that for fixed $\bar{R}$

$$\overline{D} = \frac{D}{k} \geq \frac{V_k^{-r/k}}{k+r} \exp(-r(\overline{R}-h_k)) \triangleq \overline{D}_Q^{(k)}(R), \qquad (2.54)$$

where the right-hand term will be referred to as the k-dimensional asymptotic quantizer bound. Equivalently, for fixed D we have

$$\overline{R} \geq h_k - \frac{1}{r}\log(D/k) - \frac{1}{k}\log V_k - \frac{1}{r}\log(k+r) \triangleq \overline{R}_Q^{(k)}(D). \qquad (2.55)$$

Comparing the bounds of (2.51),(2.52) and (2.54),(2.55) we have

$$\overline{R} \geq \overline{R}_Q^{(k)}(D) = \overline{R}_{SLB}^{(k)}(D) + \frac{1}{r}\log\left\{\frac{e}{1+k/r}\,\Gamma(1+k/r)^{r/k}\right\}, \qquad (2.56a)$$

$$\overline{D} \geq \overline{D}_Q^{(k)}(R) = \left\{\frac{e}{1+k/r}\,\Gamma(1+k/r)^{r/k}\right\}\overline{D}_{SLB}^{(k)}(R). \qquad (2.56b)$$

It is shown in the Appendix that the bracketed correction term above satisfies

$$\frac{e}{1+k/r}\,\Gamma(1+k/r)^{r/k} \geq 1, \qquad (2.57)$$

and hence for the asymptotic case where N or R is large or D is small, the quantizer bounds are better than those provided by the rate-distortion theory. Note that the correction term depends on the dimension and power of the seminorm but not on the particular seminorm chosen. Equations (2.56) and (2.57) generalize Gish and Pierce's [11,eq.(31)] to k dimensions and the general powers of a

seminorm.

In the special case where we use an ℓ_ν norm with $\nu = r$ and hence

$$d(\mathbf{x},\mathbf{y}) = \sum_{j=1}^{k} |x_j - y_j|^\nu$$

a single letter ν-th low distortion, if $\{\mathbf{X}_i\}_{i=0}^{\infty}$ is a stationary random process, then the rate-distortion function of the process is given by (Berger [4,ch.7])

$$R(\overline{D}) = \lim_{k\to\infty} \overline{R}^{(k)}(k\overline{D})$$

We have from Stirling's approximation that for large k

$$\left(\frac{e}{1+k/r}\right)^{k/r} \Gamma(1+k/r)$$

$$\cong \left(\frac{e}{1+k/r}\right)^{k/r} \left(\frac{1+k/r}{e}\right)^{1+k/r} \left(\frac{2\pi}{1+k/r}\right)^{1/2}$$

$$= \frac{\sqrt{2\pi}}{e} (1+k/r)^{1/2},$$

and hence from (2.56)

$$\lim_{k\to\infty} \left(\overline{R}_Q^{(k)}(k\overline{D}) - R^{(k)}(k\overline{D}) \right)$$

$$= \lim_{k\to\infty} \left((2k)^{-1} \log(1+k/r) \right) = 0,$$

or

$$\lim_{k\to\infty} \overline{R}_Q^{(k)}(k\overline{D}) = R(\overline{D})$$

and hence our lower bound asymptotically coincides with the rate-distortion function. This is not surprising since as $k \to \infty$ the performance of the optimal k-dimensional quantizers must approach the rate-distortion function if the source is stationary and ergodic (this is simply the positive source coding theorem as in Berger [4,ch.7]). This generalizes an observation of Gersho [8,eq.(31)] for the case $\nu = 2$.

2.5.3 Examples

As final examples we consider some specific source densities in order to make some numerical comparisons.

Memoryless Gaussian source

If the source is a memoryless independent identically distributed (i.i.d.) Gaussian source with marginal density

$$p(x) = \frac{1}{\sqrt{2\pi}\,\sigma} \exp\left(-\frac{x^2}{2\sigma^2}\right),$$

then the differential entropy is

$$h_k = \log(\sqrt{2\pi e}\,\sigma),$$

and for a squared-error distortion measure $d(\mathbf{x},\mathbf{y}) = \|\mathbf{x}-\mathbf{y}\|_2^2$, (2.43) becomes

$$\begin{aligned}\overline{D} = k^{-1}D &\geq k^{-1}D_L \\ &\geq \frac{1}{k+2}\cdot\frac{1}{\pi}\left(\frac{k\Gamma(k/2)}{2}\right)^{2/k} \\ &\quad \cdot \exp\left\{-\left(H_Q/k - \log(\sqrt{2\pi e}\,\sigma)\right)\right\} \qquad (2.58)\end{aligned}$$

or equivalently,

$$\begin{aligned}\frac{H_Q}{k} &\geq \frac{1}{2}\log\frac{\sigma^2}{\overline{D}} + \frac{1}{2}\log\left\{\left(\frac{2e}{k+2}\right)\left(\frac{k\Gamma(k/2)}{2}\right)^{2/k}\right\} \\ &= R_X(\overline{D}) + \frac{1}{2}\log\left\{\frac{2e}{k+2}\left(\frac{k\Gamma(k/2)}{2}\right)^{2/k}\right\}, \qquad (2.59)\end{aligned}$$

where $R_X(D)$ is the rate-distortion function of the memoryless Gaussian source. In two dimensions this becomes

$$\begin{aligned}\frac{H_Q}{2} &\geq R_X(\overline{D}) + \frac{1}{2}\log(e/2) \\ &= R_X(\overline{D}) + 0.221 \text{ [bits]} \qquad (2.60)\end{aligned}$$

We can consider the right-hand term the two-dimensional

quantization loss since it represents how far away from the rate-distortion bound we must be since we are restricted to two-dimensional block codes. In this case, however, Gersho's coefficient of quantization [8] is known exactly (the optimal decision regions are known to be hexagonal), and in this case it is known from [6],[8] that for large N one has for the optimal quantizer

$$\overline{D} \cong \frac{5}{36\sqrt{3}} \exp(-2(H_Q/2-h_2))$$

or

$$\frac{H_Q}{2} \cong R_X(\overline{D}) + \frac{1}{2}\log\left\{\left(\frac{5}{36\sqrt{3}}\right)2\pi e\right\}$$

$$= R_X(\overline{D}) + 0.227 \text{ [bits]}$$

and hence the bound (2.60) for the optimal quantizer is off from the actual asymptotic value of quantization loss by about 2.5 percent. In defense of our bound, however, the case $k = 2$ and $r = \nu = 2$ is the only case for $k > 1$ where the coefficient of quantization is known exactly and wherein the approximation can be used. The bound, however, seems tractable in quite general situations. Note also that the per-symbol entropy achievable by optimal two-dimensional quantization yields an improvement over Gish-Pierce formula [11] for one-dimensional quantization $(1/2)\log(\sigma^2/D) + 0.255$. The reduction in quantization loss resulting from two-dimensional rather than one-dimensional quantization is about 11 percent for the memoryless Gaussian source.

Memoryless Laplacian Source

Next consider the case of a memoryless source with a Laplacian marginal density,

$$p(x) = \frac{1}{\sqrt{2}\sigma} \exp\left(- \frac{\sqrt{2}|x|}{\sigma} \right)$$

(also called a double-sided exponential density). In this case

$$h_k = \log(\sqrt{2}\, e\sigma)$$

and hence, when $\nu = r = 1$, (2.43) becomes

$$\begin{aligned} \overline{D} &\geq k^{-1} D_L \\ &\geq \frac{1}{k+1} \cdot \frac{1}{2} (k\Gamma(k))^{1/k} \\ &\qquad \cdot \exp\left\{ -\left[H_Q/k - \log(\sqrt{2}\, e\sigma) \right] \right\} \\ &\geq \frac{1}{k+1} \cdot \frac{1}{2} (k!)^{1/k} \\ &\qquad \cdot \exp\left\{ -\left[H_Q/k - \log(\sqrt{2}\, e\sigma) \right] \right\} \end{aligned} \tag{2.61}$$

or

$$\begin{aligned} \frac{H_Q}{k} &\geq \log(\sqrt{2}\sigma e) - \log \overline{D} + \log \frac{(k!)^{1/k}}{2(k+1)} \\ &= \log \frac{\sigma}{\sqrt{2}\,\overline{D}} + \log \frac{e \cdot (k!)^{1/k}}{k+1} \\ &= R_X(D) + \log \frac{e \cdot (k!)^{1/k}}{k+1} \end{aligned} \tag{2.62}$$

In two dimension this becomes

$$\begin{aligned} D \geq \frac{D_L}{2} &\geq \frac{\sqrt{2}}{6} \exp(-2(H_Q/2 - \log(\sqrt{2}\sigma e)) \\ \frac{H_Q}{2} &\geq R_X(\overline{D}) + \log(e\sqrt{2}/3). \end{aligned} \tag{2.63}$$

Here we have a case where a sphere of radius r takes the form

$$\{\mathbf{u}: |u_1|+|u_2| \leq r\}$$

and such rhomboids are rotated squares which tessellate the plane [7]. Hence we can use Gersho's heuristic arguments to conjecture that for large N we can take $S_i \cong T(S_i)$ in (2.21) and hence $D \cong D_L/2$ for large N. In Gersho's terms, his coefficient of quantization for this distortion measure and $k = 2$ is given by $\sqrt{2}/6$. Thus by letting $\lambda(\mathbf{x})$ be uniform over a large bounded subset including all but the tails of the density [7], we have asymptotically that

$$\frac{H_Q}{2} \geq R_X(\overline{D}) + \log(e\sqrt{2}/3)$$

$$\cong R_X(\overline{D}) + 0.358 \text{ [bits]}$$

This compares with the one-dimensional asymptotically optimal quantizer result of

$$H_Q \cong R_X(\overline{D}) + \log(e/2)$$

$$\cong R_X(\overline{D}) + 0.443, \text{ [bits]}$$

a reduction in quantization loss of about 19 percent.

2.6 Conclusion

Gersho's bound on the asymptotic performance of vector quantizers have been genelalized to the difference distortion measures that are increasing functions of seminorm of their argument. This provides a k-dimensional generali-

zation of Gish and Pierce's results for scalar quantizers.

When the distortion measure is a power of a seminorm, the bounds were shown to be strictly better than the corresponding bounds provided by k-th order rate distortion functions.

Chapter 3

Variance Mismatch of Vector Quantizers [19],[20]

3.1 Introduction

An actual source sometimes varies its statistical properties and this causes a quantizer mismatch between a source and a quantizer. Gray and Davisson [21] derived a simple but general upper bound to the performance degradation resulting from such a quantizer mismatch. Mauersberger [22] investigated various types of quantizer mismatch by computer simulations. However, both results are limited to the scalar quantizer.

We have been discussed the optimal performance asymptotically attainable by the vector quantizer. It is not only theoretically interesting but also practically important to investigate whether the bounds derived in the previous Chapter can also be applied to evaluating the performance of mismatched vector quantizers, because the quantizer mismatch is unavoidable in practice.

In this Chapter, we derive the formula for the asymptotic performance of variance-mismatched vector quantizers. Here, the variance mismatch means the situation where a quantizer is applied to a source whose joint probability density function has the same shape but a different variance than that assumed in the design of the quantizer. We consider a generalized exponential density function, which is a multidimensional version of Miller and Thomas' density function [23], as a statistical model of sources. Our

density function includes the Gaussian density function with memory as well as the memoryless Laplacian and the memoryless Gaussian density functions as special cases.

As an example, we apply the derived asymptotic formula to the memoryless Laplacian source with the squared-error distortion measure. Computer simulations are performed to confirm the theoretical result.

Throughout this chapter we use norm-based distortion measures which are powers of an arbitrary seminorm of the error vector an in Chapter 2.

3.2 Preliminaries

In this section we summarize the fundamental concept of vector quantization, which is introduced in Chapter 2, for the convenience of our discussion.

Let $\mathbf{X}$ be a k-dimensional random vector described by a joint probability density function $p(\mathbf{x})$, where $\mathbf{x} = (x_1, x_2, \ldots, x_k) \in R^k$, and R^k is k-dimensional Euclidean space. A vector quantizer with block length k and codebook rate R is defined by a collection of $N = 2^R$ reproduction vectors $\mathbf{y}_1, \mathbf{y}_2, \ldots, \mathbf{y}_N \in R^k$, called the reproduction alphabet, and by a partition $(S_1, S_2, \ldots S_N)$ of R^k.

The vector quantizer Q is defined by

$$Q(\mathbf{x}) = \mathbf{y}_i, \quad \text{if} \quad \mathbf{x} \in S_i. \tag{3.1}$$

Given a reproduction alphabet $\{\mathbf{y}_i\}$, the corresponding partition $\{S_i\}$ can be defined by the nearest neighbor (or minimum distortion) rule such that, for any vector $\mathbf{x} \in S_i$,

the distance (distortion) between $\mathbf{x}$ and $\mathbf{y}_i$ is less than or equal to the distances (distortions) between $\mathbf{x}$ and $\mathbf{y}_j$ ($j \neq i$; $i,j=1,2,\ldots,N$). Ties can be broken in any arbitrary prescribed manner without increasing distortion. Roughly speaking, each quantizer input vector will be quantized and reproduced as the nearest reproduction vector.

The distortion resulting from reproducing a vector $\mathbf{x}$ as $\mathbf{y}$ is measured throughout this Chapter by the following norm-based distortion measure,

$$d(\mathbf{x},\mathbf{y}) = \|\mathbf{x}-\mathbf{y}\|^r , \quad r \geq 1, \tag{3.2}$$

where $\|\cdot\|$ denotes an arbitrary seminorm on $\mathbf{R}^k$. The distortion must be based on the seminorm of the error vector $\mathbf{x} - \mathbf{y}$ in order to apply the lower bound, which has been developed in Chapter 2.

Figure 3.1 demonstrates examples of the waveforms of the source output, the waveform produced by the optimal scalar quantizer, and the waveforms produced by the locally optimal vector quantizers with k = 2 and 4. In Fig. 3.1, the memoryless Laplacian source and the squared-error distortion measure are assumed. It is seen that the details of the waveforms produced by the vector quantizers with longer block lengths resemble more closely the detail of the original waveform, although all the quantizers used in Fig. 3.1 (b)-(d) have the same per-symbol codebook rate, $\overline{R} = R/k = 2$ [bits]. More precisely, for k = 1, 2, and 4, we have R = 2,4, and 8 [bits] respectively, and thus $\overline{R} = R/k = 2/1 = 4/2 = 8/4 = 2$ [bits].

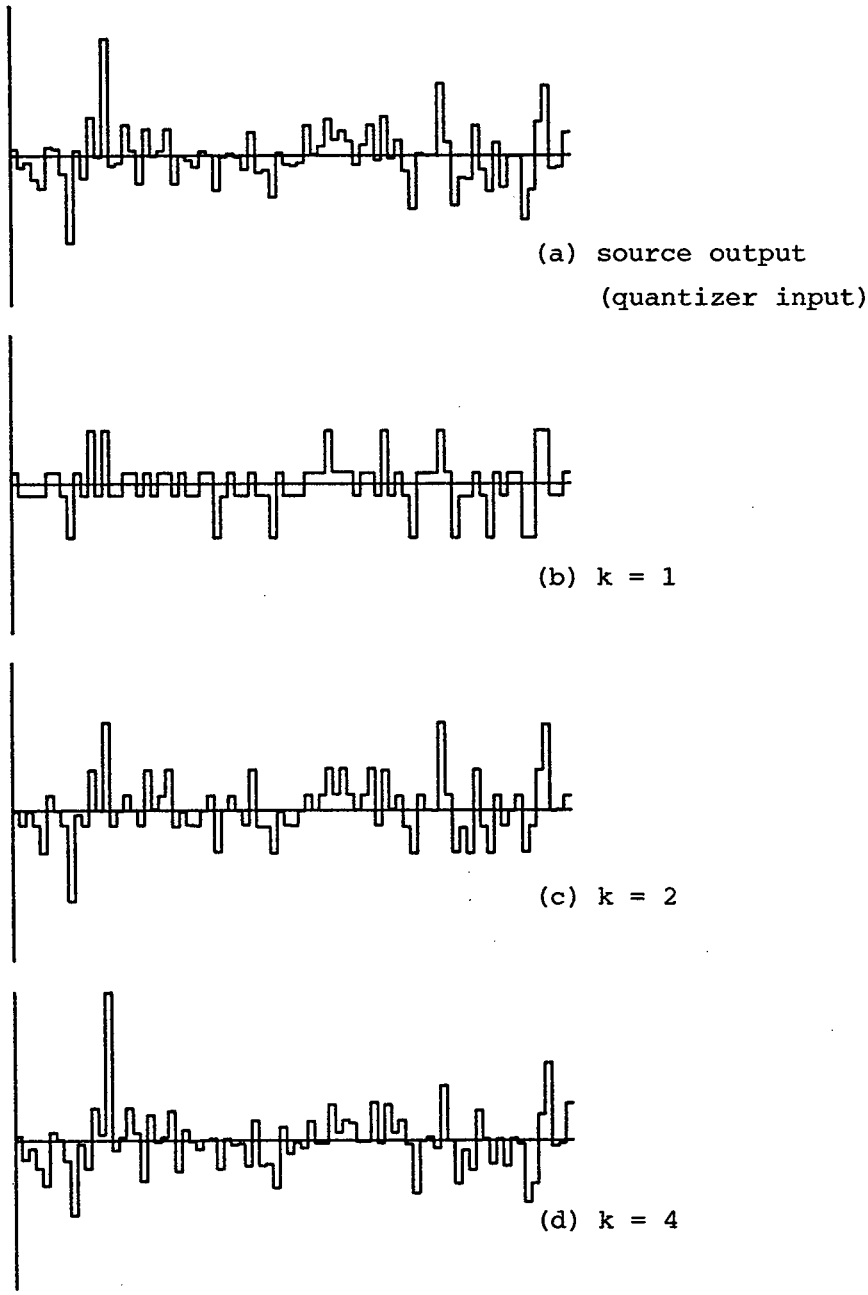

Fig. 3.1 Examples of the waveforms quantized by the optimal quantizers with k = 1,2, and 4 ($\overline{R}$ = 2).

We now consider the vector quantizer described by the reproduction alphabet in which N reproduction vectors are produced randomly with a reproduction vector density $\lambda(\mathbf{x})$, which can be related to the k-dimensional volume

$$V(S_i) = \int_{S_i} d\mathbf{x}$$

of the atom S_i as follows:

$$\lambda(\mathbf{x}) \cong \frac{1}{N \cdot V(S_i)}, \quad \mathbf{x} \in S_i.$$

For N large, most of the atom S_i will be bounded and the overload region will correspond to the tail of the density $p(\mathbf{x})$. Hence, we can replace N by the number of bounded atoms.

As seen in Chapter 2, the average distortion $D = E\{d(\mathbf{X},Q(\mathbf{X}))\}$ obtainable by the vector quantization with the reproduction vector density $\lambda(\mathbf{x})$ can be bounded asymptotically as follows:

$$D \geq D_L = \frac{k}{k+r} V_k^{-r/k} 2^{-r\overline{R}} E\left\{\lambda(\mathbf{X})^{-r/k}\right\}, \qquad (3.3)$$

where

$$V_k = \int_{\|\mathbf{x}\| \leq 1} d\mathbf{x} \qquad (3.4)$$

is the k-dimensional volume of the sphere of unit radius as measured by the given seminorm $\|\cdot\|$. We assume that V_k is finite.

Applying Hölder's inequality to (3.3), we have obtained

$$D_L \geq \frac{k}{k+r} V_k^{-r/k} \, 2^{-r\overline{R}} \| p \|_{k/(k+r)} ,$$

where here the norm denotes the $L_{k/(k+r)}$ norm on real function defined on R^k. The equation above holds in equality if and only if the reproduction vector density $\lambda(\mathbf{x})$ is proportional to $p(\mathbf{x})^{k/(k+r)}$. Consequently, the optimal reproduction vector density $\lambda_o(\mathbf{x})$, which minimizes D_L, is given by

$$\lambda_o(\mathbf{x}) = \frac{p(\mathbf{x})^{k/(k+r)}}{\int p(\mathbf{x})^{k/(k+r)} \, d\mathbf{x}} .$$

Using (3.3) we shall evaluate the average distortion obtainable by variance-mismatched vector quantizers.

3.3 Statistical Model of Sources

3.3.1 Generalized Exponential Density

We consider a generalized exponential density function, which is a multidimensional version of Miller and Thomas' density function [23] and is given by

$$p(\mathbf{x}) = \frac{\xi^{k/s}}{W_k \cdot \Gamma(1+k/s)} \exp\left\{ -\xi \| \mathbf{x} \|^s \right\}, \qquad (3.5)$$

where $\| \cdot \|$ denotes an arbitrary seminorm on R^k, and W_k denotes the k-dimensional volume defined by

$$W_k = \int_{\| \mathbf{x} \| \leq 1} d\mathbf{x} . \qquad (3.6)$$

The volume W_k is also assumed to be finite. We see that the parameter ξ (>0) is inversely proportional to the s-th

power of the standard deviation of the random variable $\|\mathbf{x}\|$. More precisely, we have

$$E\left\{\|\mathbf{x}\|^2\right\} = \frac{\Gamma((k+2)/s)}{\Gamma(k/s)}\,\xi^{-2/s} \quad .$$

The parameter s (> 0) will be referred to as the shape parameter.

The new notation for the seminorm, $\|\cdot\|$ used to avoid confusion between the possibly different norms in (3.2) and (3.5). The seminorm $\|\cdot\|$ specifies the shape of the probability density function of the source output vector and is not neccessarily same as the seminorm $\|\cdot\|$ which specifies the distortion measure.

3.3.2 Examples

To make our discussion more understandable, we shall give some examples of the density function defined in (3.5).

Memoryless Laplacian source

$$p(\mathbf{x}) = (\xi/2)^k \exp\left\{-\xi \|\mathbf{x}\|_1\right\}, \qquad (3.7)$$

where $\|\cdot\|_1$ is the ℓ_1 norm. The shape parameter s is set equal to unity.

Memoryless Gaussian source

$$p(\mathbf{x}) = (\xi/\pi)^{k/2} \exp\left\{-\xi \|\mathbf{x}\|_2^2\right\}, \qquad (3.8)$$

where $\|\cdot\|_2$ is the ℓ_2 norm. The shape parameter is $s = 2$.

Gaussian source with memory

$$p(\mathbf{x}) = \sqrt{(\xi/\pi)^k \det \mathbf{B}}\ \exp\left\{-\xi \|\mathbf{x}\|_{\mathbf{B}}^2\right\}, \quad (3.9)$$

where det **B** denotes the determinant of the k x k symmetric nonnegative matrix $\mathbf{B} = [B_{ij}]$, and $\|\cdot\|_{\mathbf{B}}$ is the quadratic norm of the form,

$$\|\mathbf{x}\|_{\mathbf{B}} = \sqrt{\mathbf{x}\mathbf{B}\mathbf{x}^t} = \sqrt{\sum_{i=1}^{k}\sum_{j=1}^{k} x_i x_j B_{ij}}\ . \quad (3.10)$$

The shape parameter is $s = 2$. In (3.10), $\mathbf{x}^t$ denotes the transpose of **x**.

3.4 Bounds on Asymptotic Performance

3.4.1 Variance Mismatch

Observe that if we assume the generalized exponential density as the source density then the optimal reproduction vector density $\lambda_o(\mathbf{x})$ is given by the scaled version of the source density $p(\mathbf{x})$ as follows:

$$\lambda(\mathbf{x}) \sim p(\mathbf{x})^{k/(k+r)} \sim \exp\left\{-\frac{k\cdot\xi}{k+r}\|\mathbf{x}\|^s\right\}.$$

Note that again the optimal reproduction vector density $\lambda_o(\mathbf{x})$ has the same shape as the source density $p(\mathbf{x})$, (3.5), but differs in variance. This means that, in this case, the variance mismatch can be modeled mathematically as the mismatch in variance between the source density $p(\mathbf{x})$ and the reproduction density $\lambda(\mathbf{x})$, which is given by

$$\lambda(\mathbf{x}) = \frac{\eta^{k/s}}{W_k \Gamma(1+k/s)} \exp\left\{-\eta \|\mathbf{x}\|^s\right\}. \qquad (3.11)$$

From (3.5) and (3.11), we obtain

$$E\left\{\lambda(\mathbf{X})^{-r/k}\right\}$$
$$= \left\{W_k \Gamma(1+k/s)\right\}^{r/k} \cdot \eta^{-r/s} \cdot \left\{1 - \frac{r}{k}\cdot\frac{\eta}{\xi}\right\}^{-k/s}$$
$$; \quad 1 - r\eta/k\xi > 0. \qquad (3.12)$$

Substituting (3.12) into (3.3), and multiplying both sides of the equation by $\xi^{r/k}$, we have the following lower bound for the average distortion obtainable by mismatched vector quantizers.

$$\xi^{r/s} D_L = \frac{k}{k+r} 2^{-r\bar{R}} \left\{\frac{W_k}{V_k} \Gamma(1+k/s)\right\}^{r/k}$$
$$\cdot \left\{f\left(\frac{\eta}{\xi}, \frac{k}{r}\right)\right\}^{-r/s} \quad ; \quad 1-r\eta/k\xi > 0, \qquad (3.13)$$

where

$$f(t,a) = t\cdot(1-t/a)^a \quad ; \quad t < a \qquad (3.14)$$

is the <u>degradation factor</u>, which represents the performance degradation due to the variance mismatch, and

$$\lim_{a\to\infty} f(t,a) = t\cdot\exp(-t) \geq f(t,a).$$

For a given a, the degradation factor $f(t,a)$ has maximum value $[a/(a+1)]^{a+1}$ at $t = a/(a+1)$. Consequently, $f(\eta/\xi, k/r)^{-r/s}$ has its miminum value $[k/(k+r)]^{-(k+r)/s}$ when $\eta/\xi = k/(k+r)$. This is the natural result of the fact that a $\lambda(\mathbf{x})$ proportional to $p(\mathbf{x})^{k/(k+r)}$ is the optimal reproduction vector density function.

3.4.2 Example of Bound

Consider the squared-error distortion measure,

$$d(\mathbf{x},\mathbf{y}) = \|\mathbf{x}-\mathbf{y}\|_2^2 \tag{3.15}$$

For this distortion measure, we have [15,p.620]

$$V_k = \frac{\pi^{k/2}}{\Gamma(1+k/2)}, \tag{3.16}$$

where the unit length is measured by the l_2 norm.

For the memoryless Laplacian source (3.7), we have [15]

$$W_k = \frac{2^k}{\Gamma(1+k)}, \tag{3.17}$$

where the unit length is measured by l_1 norm.

Substituting (3.16) and (3.17) into (3.13), we obtain

$$\frac{D_L}{\sigma_\xi^2} = \frac{k\, 2^{-2\overline{R}}}{\pi(1+k/2)} \cdot \left\{\Gamma(1+k/2)\right\}^{2/k} \cdot \left\{f\left(\frac{\sigma_\xi}{\sigma_\eta}, \frac{k}{2}\right)\right\}^{-2} ; \quad k/2 > \sigma_\xi/\sigma_\eta, \tag{3.18}$$

where $\sigma_\xi = \sqrt{2}/\xi$ and $\sigma_\eta = \sqrt{2}/\eta$ are the standard deviations of the marginal density functions of $p(\mathbf{x})$ and $\lambda(\mathbf{x})$, respectively. We shall refer to σ_ξ^2 and σ_η^2 as the variances of the source output and the reproduction alphabet, respectively.

In the asymptotic situation where $k \to \infty$, we have from (3.18),

$$\lim_{k\to\infty} \frac{D_L}{k\sigma_\xi^2} = \frac{2^{-2\overline{R}}}{\pi}\left(\frac{\sigma_\xi}{\sigma_\eta}\right)^{-2} \exp\left\{2\left(\frac{\sigma_\xi}{\sigma_\eta}\right) - 1\right\}$$

$$\geq \frac{e}{\pi}\, 2^{-2\overline{R}} = \overline{D}_{SLB}(\overline{R})/\sigma_\xi{}^2 \tag{3.19}$$

Equality holds in the right-hand inequality of (3.19) when

$\sigma_\xi = \sigma_\eta$. In (3.19), $\overline{D}_{SLB}(\overline{R})$ denotes the Shannon Lower Bound for the memoryless Laplacian source with the squared-error distortion measure and can be easily obtained, for example, from (4.3.1) of [4].

The relationships between $D_L/k\sigma_\xi^2$ and $(\sigma_\xi/\sigma_\eta)^2$ is calculated from (3.18) with k = 1, 2, 4, 8, and ∞, and shown in Fig. 3.2. The minima of the distortions become broader as k increases. This means that well-designed vector quantizers

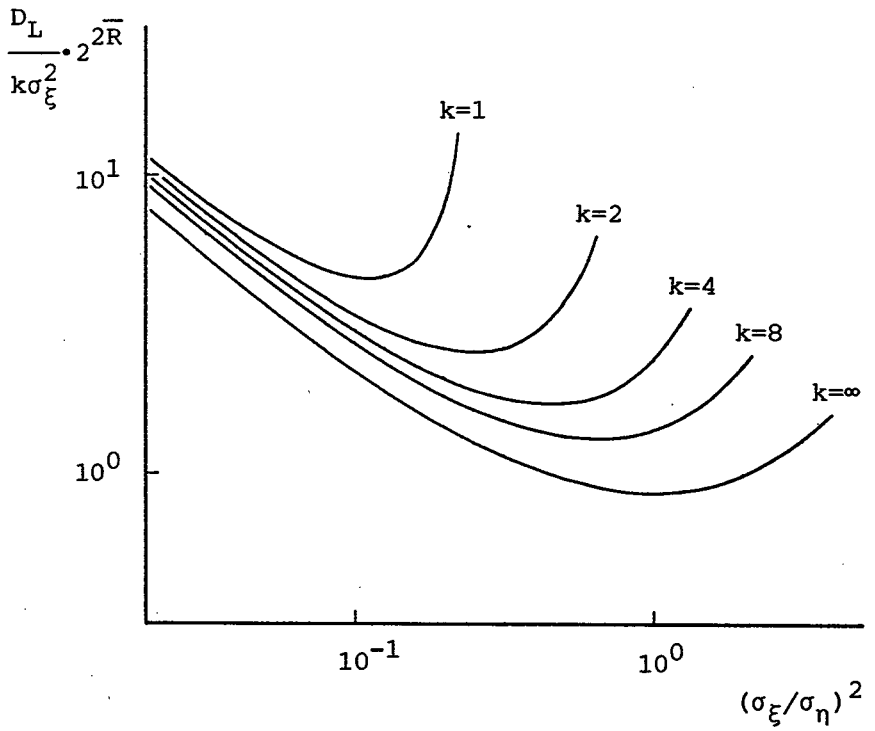

Fig. 3.2 Average distortion resulting from variance-mismatched vector quantizers.

are inherently invulnerable to variance mismatch compared with conventional scalar quantizers. It is interesting to note that the value of σ_ξ/σ_η that gives the minimum depends on the block length k, and approaches unity as k increases. That is, the reproduction alphabet with variance σ_η^2 optimally matches with the source with the variance

$$\sigma_\xi^2 = \left\{\frac{k}{k+r}\right\}^2 \sigma_\eta^2.$$

In the asymptotic case where k is sufficiently large, the reproduction alphabet whose variance is equal to that of the source output (quantizer input) gives a nearly optimal vector quantizer.

3.4.3 Comparison with Simulations

Computer simulations were performed using the locally optimal quantizers with block lengths k = 1,2, and 4. The iterative optimization methods [24] are used for obtaining the quantizers assuming that the variance of the source output is unity. The codebook rate per block R of all quantizers equals 8 [bits], and therefore $\overline{R}$ = 8, 4, and 2 bits per sample for k = 1, 2, and 4-dimensional quantizers, respectively. The results, $D_L/k\sigma_\xi^2$ versus $(\sigma_\xi/\hat{\sigma}_\eta)^2$, are shown in Fig. 3.3, where

$$\hat{\sigma}_\eta^2 = \left\{\frac{k+r}{k}\right\}^2$$

is the variance of the optimal reproduction vector density

for the source with unit variance. In Fig. 3.3, the theoretical bounds are also shown. It seems that approximately $k\overline{R}$ = 6 to 8 bits per block are required to ensure the tightness of the lower bound. From Fig. 3.3, we can conclude that the asymptotic bounds (3.13) and (3.18) for sufficiently large $N = 2^R$ give good bounds of the performance of variance-mismatched vector quantizers provided that the overload is negligible.

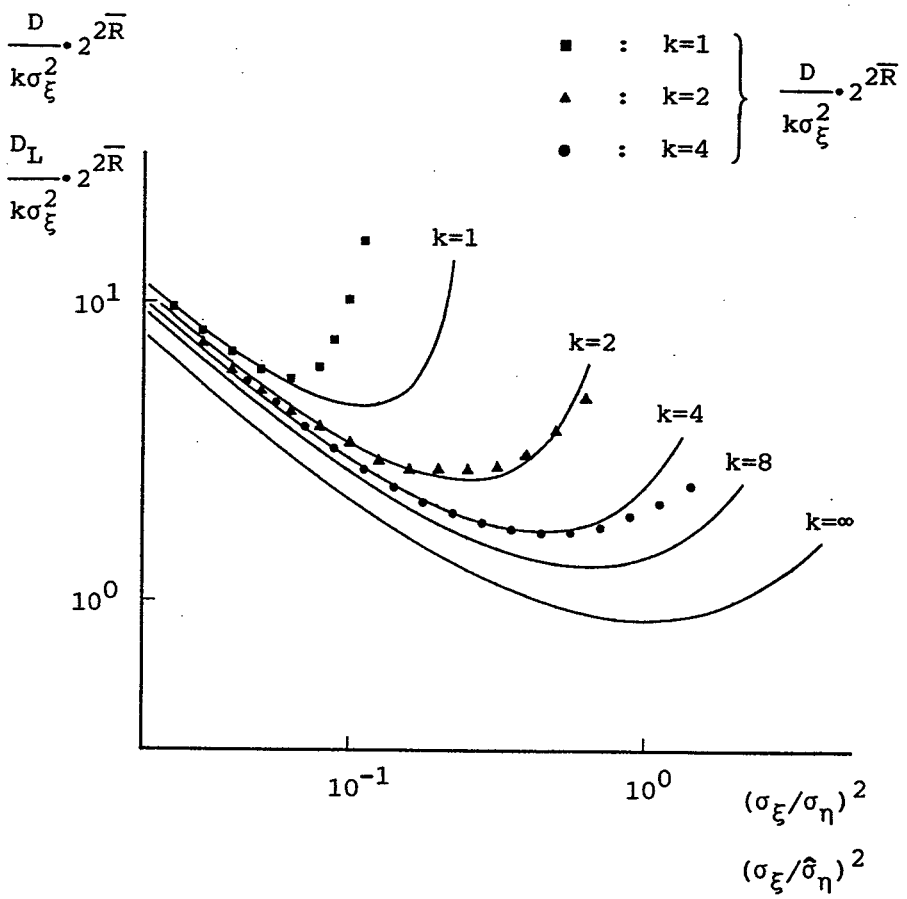

Fig. 3.3 Results of simulations.

3.5 Conclusion

The asymptotic performance of variance-mismatched vector quantizers was derived for distortion measures that are r-th powers of a seminorm of the error vector. It was shown that the performance degradation due to the variance mismatch can be expressed by the simple degradation factor. This asymptotic bound was then applied to the memoryless Laplacian source with the squared-error distortion measure. As a result, through both asymptotic analysis and computer simulations, we have found the interesting fact that well-designed vector quantizers are more invulnerable to the mismatch than are conventional scalar quantizers.

Chapter 4

Vector Quantization of Video Signals [25]-[27]

4.1 Introduction

Video signals as well as speech signals have been acting the leading role in man-to-man and man-to-machine interfaces. Since the information contents of the video signals are approximately one thousand times that of the speech signals, the data compression is essential in the future information network systems.

In the past two decades, a number of approaches and techniques are proposed and developed for efficient data compression of video signals [28]. For example, the transform coding and the predictive coding are well known as standard data compression techniques in the textbook of this field [1].

These data compression systems are employing one or more scalar quantizers for analog-to-digital conversion. From the information-theoretical point of view, the scalar quantizers provide rather poor performance for relatively low information rate, approximately one bit per symbol or less, whereas they provide good performance when large information rate is allowed. As we discussed in the previous Chapters, the vector quantizers can provide nearly optimal performance when the block length is sufficiently large.

In this Chapter, we discuss the vector quantization of video signals. Based on the asymptotic analysis in Chapter 2, the vector quantizers with several norm-based distortion

measures are investigated. Computer simulations are performed to demonstrate the effectiveness of the vector quantization for real video signals.

4.2 Preliminaries

The asymptotic performance of vector quantizers with difference distortion measures has been studied in the previous Chapters. One of the principal results in Chapter 2, Eq.(2.38), states that the optimal reproduction vector density $\lambda_o(\mathbf{x})$ is proportional to $p(\mathbf{x})^{k/(k+r)}$, where $p(\mathbf{x})$ is the source density. Here the norm-based distortion measure

$$d(\mathbf{x},\mathbf{y}) = \|\mathbf{x}-\mathbf{y}\|^r \quad , \quad r \geq 1$$

and the codebook rate $R = \log N$, where N is the number of the vectors in the reproduction alphabet, are assumed. As seen in Chapter 3, $\lambda_o(\mathbf{x})$ can be expressed as

$$\lambda_o(\mathbf{x}) = \frac{p(\mathbf{x})^{k/(k+r)}}{\int p(\mathbf{x})^{k/(k+r)}\, d\mathbf{x}} .$$

In the asymptotic situation, where k is sufficiently large, the source density $p(\mathbf{x})$ is the optimal reproduction vector density itself.

Here, we shall give some interpretation of this statement. An optimistic interpretation may be as follows:

"If the source is sufficiently stationary, a set of sample vectors, extracted from the source output, will provide the nearly optimal reproduction alphabet."

This intuitive interpretation is the case when k and $N = 2^R$ are sufficiently large. However, it is too optimistic to apply this method to the real video signals, since the real video signals are far from stationary. In a word, it is very suggestive but not feasible.

We must note the fact that the optimal reproduction vector density does not depend on the norm selected to define the corresponding distortion measures. This suggests that "the difference between the distribution of the reproduction alphabets which are optimized assuming the different distortion measures, e.g. d_A or d_B, diminishes as k increases." In other words, these two reproduction alphabets are equivalent in the sense that they provide very near performance (average distortion). This allows us to use an alternative distortion measure d_A, which is easy to implement or less complex, instead of the distortion measure d_B which is, for some reason, suitable for the combination of the source and the destination but more complex.

4.3 Quantization with Several l_ν Norms

4.3.1 Distortion Measures and Norms

We now consider the computational complexity in evaluating the distortion or distance between two vectors. In this Chapter, we confine ourselves to the norm-based distortion measures that are powers of l_ν norms. That is, reproducing a vector **x** as a vector **y** is assumed to yield the distortion

$$d(\mathbf{x},\mathbf{y}) = \|\mathbf{x}-\mathbf{y}\|_\nu^r , \quad r \geq 1$$

where $\| \cdot \|_\nu$ is an arbitrary l_ν norm.

From the practical point of view, there are three important norm-based distortion measures:

$$d_1(\mathbf{x},\mathbf{y}) = \|\mathbf{x}-\mathbf{y}\|_1 = \sum_{j=1}^{k} | x_j - y_j | \qquad (4.1)$$

$$d_2(\mathbf{x},\mathbf{y}) = \|\mathbf{x}-\mathbf{y}\|_2^2 = \sum_{j=1}^{k} (x_j - y_j)^2 \qquad (4.2)$$

$$d_\infty(\mathbf{x},\mathbf{y}) = \|\mathbf{x}-\mathbf{y}\|_\infty = \max_{1 \leq j \leq k} | x_j - y_j | \qquad (4.3)$$

We shall refer to d_1, d_2, and d_∞ as the absolute, squared and maximum error distortion measures in the rest of this Chapter. Other norm-based distortion measures require more complicated computation/operation than that these three distortion measures do.

The absolute error distortion measure uses l_1 norm, which requires the subtraction, taking an absolute value, and summation (accumulation). The squared error distortion measure uses l_2 norm, which requires the subtraction, multiplication, and summation. The maximum error distortion measure uses l_∞ norm, which requires the subtraction, taking an absolute value, and taking a maximum value. From the observation above, it is easy to conclude that the squared error distortion measure d_2 is the most complex of these three distortion measures. Moreover the multiplication needs longer precision than other operations, e.g. subtraction and addition. The maximum error distortion measure d_∞ is the least complex of the three since the intermediate precision is the same as that of operands

and less than that of d_1, although both distortion measures need no multiplications.

We employ in the rest of this Chapter, the mean-squared-error (MSE) fidelity criterion to evaluate the performance of the vector quantizers, where the average distortion D means the average of the squared error distortion d_2, that is $D = E\{d_2(\mathbf{x},Q(\mathbf{x}))\}$, although the distortion measure used in the quantization operation may possibly be d_1, d_2, or d_∞.

4.3.2 Comparison under the MSE Fidelity Criterion

We shall give two examples to demonstrate the validity of the statement as discussed in the previous section.

Consider the memoryless Laplacian source with zero mean and unit variance as an example of the source to be quantized. Let $Q_1^{(k)}$ and $Q_2^{(k)}$ denote the k-dimensional vector quantizers which are optimized assuming the absolute error distortion measure d_1 and the squared error distortion measure d_2, respectively. The subscripts "1" and "2" are from the norms on which the distortion measures are based, i.e. d_1 and d_2 are based on ℓ_1 and ℓ_2 norms, respectively. Note that, when $k = 1$, $Q_1^{(k)}$ and $Q_2^{(k)}$ are scalar quantizers. The performance of $Q_2^{(1)}$ was discussed by Paez et al. [29]. Table 1 shows the performance (MSE) of the quantizers $Q_1^{(k)}$ and $Q_2^{(k)}$ when the per-symbol codebook rate $\overline{R} = 2$ [bits]. These quantizers are obtained by using the iterative optimization method [24]. Since the mean-squared-error fidelity criterion is employed, the quantizer

$Q_2^{(k)}$ are the optimal quantizers for each block length k. The quantizers $Q_1^{(k)}$ are not optimal since they are optimized employing mean-absolute-error fidelity criterion. It is seen that the average distortion obtained by the quantizer $Q_1^{(k)}$ approaches to that is obtained by the quantizer $Q_2^{(k)}$ as k increases This proves that the statement as discussed in the Pleliminaries are valid for k small.

Table 4.1 MSE obtained by $Q_1^{(k)}$ and $Q_2^{(k)}$ ($\overline{R} = 2$).

k	1	2	3	4
MSE obtained by $Q_1^{(k)}$	0.210	0.155	0.113	0.111
MSE obtained by $Q_2^{(k)}$	0.178	0.135	0.115	0.106

The second example is on the special case of $Q_2^{(k)}$ when k = 2. Figure 4.1 shows the reproduction alphabet, which contains $2^{k\overline{R}} = 16$ vectors, of the two-dimensional vector quantizer $Q_2^{(2)}$. Figure 4.2 illustrates the corresponding optimal or minimum distortion partitions when the distortion measures d_1, d_2, and d_∞ are employed, respectively. Of course, the partition based on d_2 is optimal since MSE fidelity criterion is assumed. Although these partitions seem to be very different, the average distortion obtained by these quantizers, the combinations of the reproduction

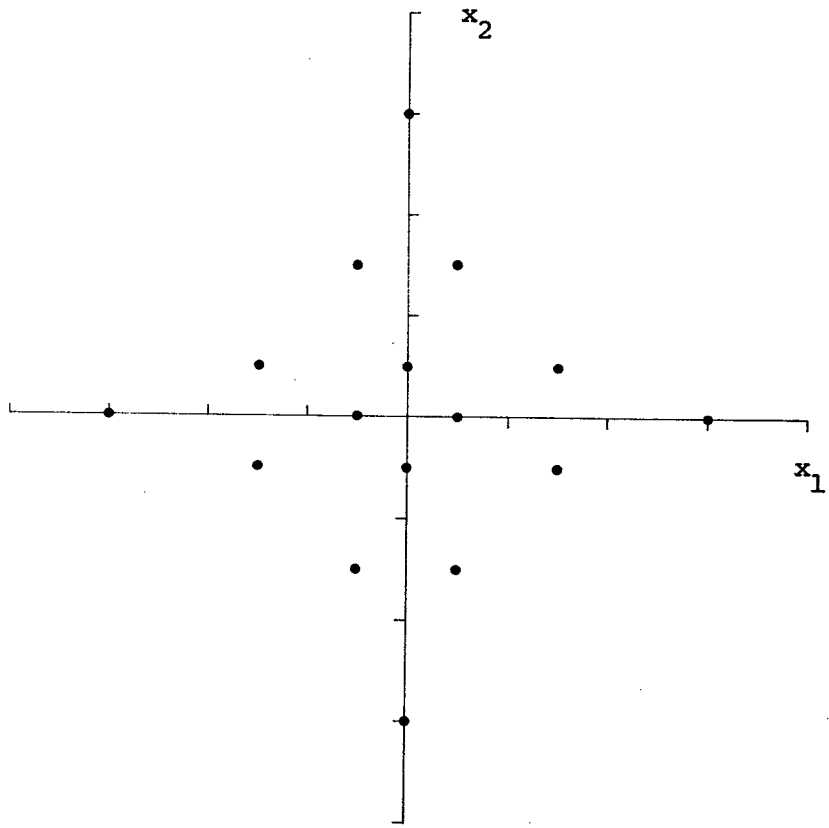

Fig. 4.1 Reproduction alphabet of $Q_2^{(2)}$ ($\overline{R} = 2$).

In the figure above and also in the figures in page 56-58, Figs. 4.1 - 4.4, the reproduction vectors are represented by the symbol "•".

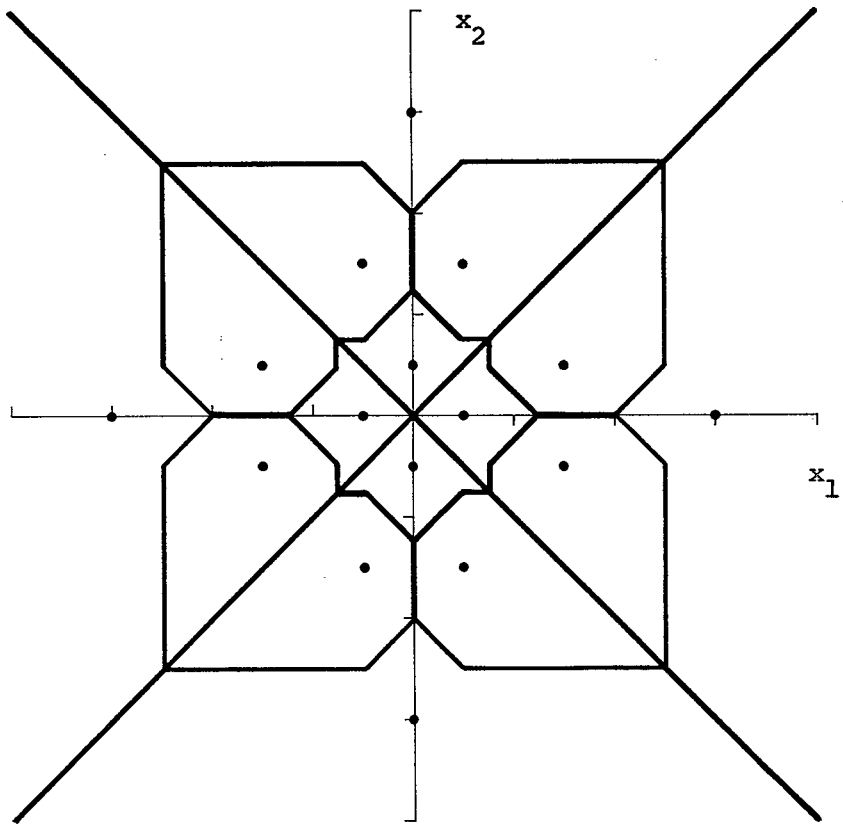

(a) d_1

Fig. 4.2 Partitions based on d_1, d_2, and d_∞.

In Figs. 4.2-4.4, the same reproduction alphabet is used, as shown in Fig. 4.1, but the partitions are different since they are determined by the different distortion measures, namely d_1, d_2, and d_∞, respectively.

(continued)

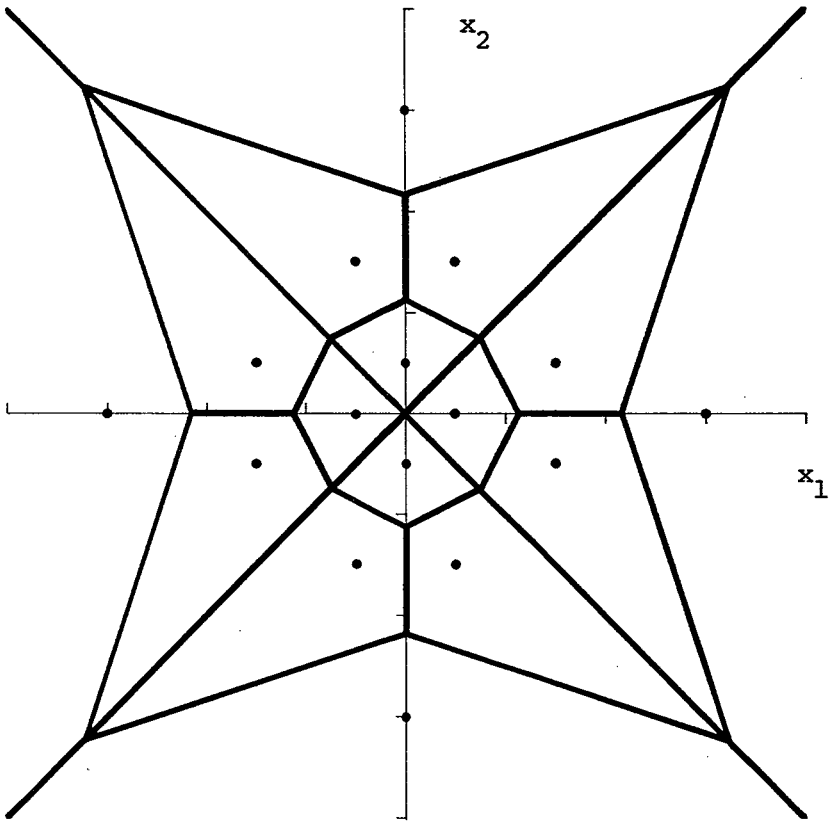

(b) d_2

Fig. 4.2 Partitions based on d_1, d_2, and d_∞.

(continued)

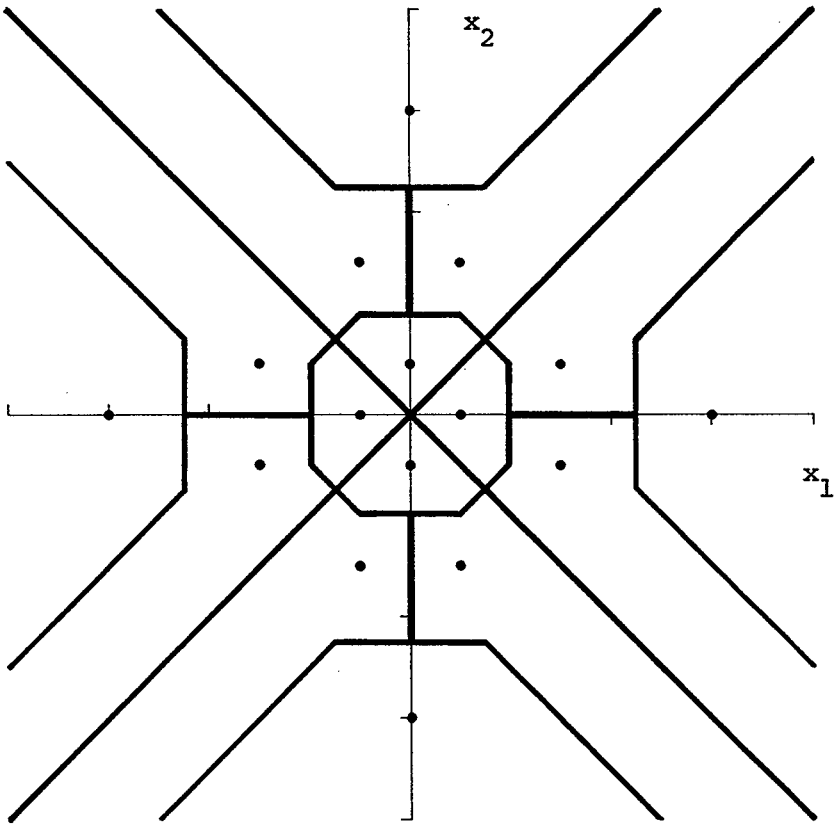

(c) d_∞

Fig. 4.2 Partitions based on d_1, d_2, and d_∞.

alphabet and the partitions, are quite similar as shown in Table 4.2. The average distortions, when the partitions in Fig. 4.2 (a) and (c) are used, are atmost 2 percent greater than that given by the partition in Fig. 4.2 (b).

Table 4.2 MSE obtained by the partitions based on d_1, d_2, and d_∞.

distortion measures	d_1	d_2	d_∞
Partitions	(a)	(b)	(c)
MSE	0.1374	0.1352	0.1377

It can be concluded, from these examples, that the statement that the optimal reproduction density does not depend on the norm selected to define the distortion measure is true even if the block length k is relatively small. It seems that k = 4 is sufficient to make this true.

4.3.3 Centroids

The locally optimal vector quantizers can be designed by the iterative optimization method [24], which is summarized as follows:

(1) Guess an initial reproduction alphabet. Set D_{old} infinity. Set δ positive nonzero value for terminating the iteration when the average distortion converges.

(2) Obtain the optimal partition which minimizes the average distortion for given reproduction alphabet.

(3) Obtain the optimal reproduction alphabet which minimizes the average distortion for given partition.

(4) Calculate the average distortion D_{new}. If

$$1 - D_{new}/D_{old} < \delta,$$

then stop, else substituting D_{new} into D_{old}, go to (2).

Note that the average distortion D_{new} converges monotonously provided that the partition in the step (2) and the reproduction alphabet in the step (3) are the optimal for given reproduction alphabet and partition, respectively [24].

The optimization is done, in general, by using "training sequence", which is a sample sequence produced by the source to be quantized or a pseudo-random sequence when the source is a random source, e.g. Gaussian source. One of the reasons why the calculation is based on the training sequence instead of the statistical model of the source is from the difficulty of the multi-dimensional integrations to be performed for obtaining the centroids in the step (3). Another reason is from the difficulty in modeling the video signals.

In the step (2), the partition is determined equivalently by searching the nearest reproduction vector to a given training vector, since it is too difficult to determine the optimal partition explicitly in the multi-dimensional space. The operation to be performed in this step is "vector quantization" itself. In the step (3), the optimal reproduction alphabet is obtained by calculating the

centroid in each atom.

Here we compare the computational complexity for calculating the centroids in the step (3).

For the absolute error distortion measure, the centroid can be represented in the continuous (or integral) form by the set of solutions of the following equations.

$$\int_{\substack{x\in S_i \\ x_j \leq y_{ij}}} p(\mathbf{x})\,d\mathbf{x} = \int_{\substack{x\in S_i \\ x_j > y_{ij}}} p(\mathbf{x})\,d\mathbf{x}$$

$$; \; j=1,2,\ldots,k. \qquad (4.4)$$

Equation (4.4) shows that the j-th component of the reproduction vector $\mathbf{y}_i$ is given by the median in the atom S_i.

For the squared-error distortion measure, the centroid in the atom S_i can be given explicitly by

$$\mathbf{y}_i = \frac{\int_{x\in S_i} \mathbf{x}p(\mathbf{x})\,d\mathbf{x}}{\int_{x\in S_i} p(\mathbf{x})\,d\mathbf{x}} . \qquad (4.5)$$

In this case, the centroid $\mathbf{y}_i$ is only the mean vector in the atom S_i.

For the maximum-error distortion measure, the centroid can be represented by the solutions of the following simultaneous nonlinear equations, however it cannot be solved explicitly and it seems far from tractable.

$$\frac{\partial}{\partial \mathbf{y}_i} \int_{x\in S_i} \| \mathbf{x}-\mathbf{y}_i \|_\infty \, p(\mathbf{x})\,d\mathbf{x} = 0 . \qquad (4.6)$$

Comparing Eqs. (4.4)-(4.6), it is easily seen that the centroid for d_2 is least complex, the centroid for d_1 is more complex than that for d_2 but computable, and the centroid for d_∞ is the most complex of these examples. Thus, in the step (3), d_2 is preferable, whereas in the step (2) d_∞ is preferable as discussed in 4.3.1.

Here we have the following question:

"When we use d_∞ in the step (2) and d_2 in the step (3), does the average distortion calculated in the step (4) converge?"

Figure 4.3 illustrates the answer by an example of this question, wherein the block length k = 2 and the per-symbol codebook rate is $\overline{R} = 2$. This Figure compares the convergence of the average distortion D_{new} in each iteration, when d_∞ or d_2 is used in the step (2). In the step (3), d_2 is always used. It is found from the Figure that, even if d_∞ is used in the step (2), the average distortion converges to that of approximately 3 percent greater than that obtained by using d_2.

Thus, from these examples, we can conclude that the maximum error distortion measure can be used for relaxing the computational complexity of the vector quantization even when the fidelity criterion is based on the mean-squared-error.

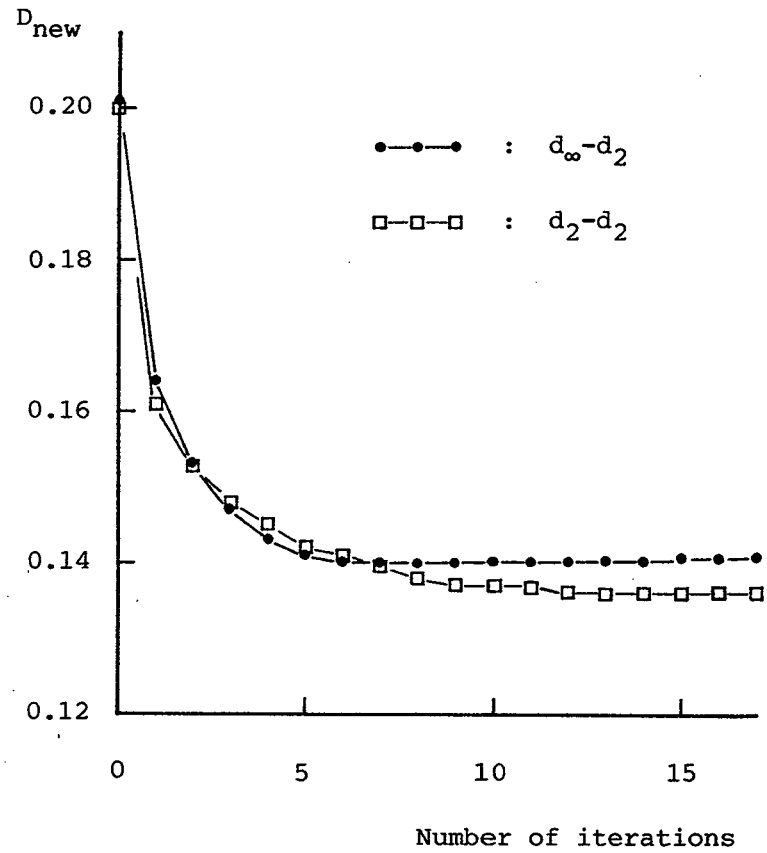

Fig. 4.3 Convergence of the average distortion D_{new}.

In Fig. 4.3, d_∞-d_2 represents that d_∞ is used in the step (2) and d_2 is used in the step (3). Similarly, d_2-d_2 represents that, in both steps (2) and (3), only d_2 is used. In both cases, the average distortion means the MSE. At the "0"-th iteration in the Figure, D_{new} shows the average distortion for the initial reproduction alphabet.

4.4 Simulations

4.4.1 Quantizer Design

In the following simulations, two image data are used as samples of real video signals. One of them, is referred to as GIRL (Ver. 002, No. 1), and the other HOME (Ver. 003, No. 26) [30]. These original image data are shown in Fig. 4.4.

The locally optimal vector quantizers are designed by the method as described in the previous section. The quantizer input vector $\mathbf{x}$ is assumed to be composed by 4 x 4 picture elements as shown in Fig. 4.5, where the symbol "+" denotes a picture element.

The Signal-to-Noise Ratio (SNR) is defined as follows:

$$SNR = 20 \log_{10} \left(\frac{S_{p-p}}{N_{rms}} \right), \quad [dB]$$

where S_{p-p} denotes the peak-to-peak of the video signals, and N_{rms} denotes the per-symbol root-mean-square of the quantization error. Here, S_{p-p} is assumed to be $2^8 - 1 = 255$ for convenience, since the original image data are of 8-bit resolution of gray scale. The denominator N_{rms} is defined by

$$N_{rms} = \sqrt{k^{-1} E\left\{ d_2(\mathbf{X}, Q(\mathbf{X})) \right\}} \ .$$

(a) GIRL

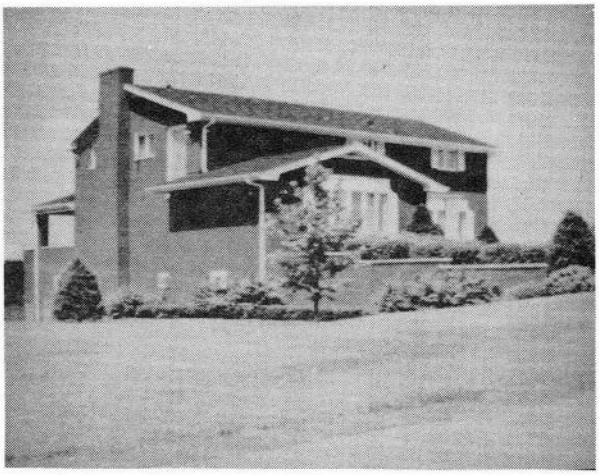

(b) HOME

Fig. 4.4 Original Images.

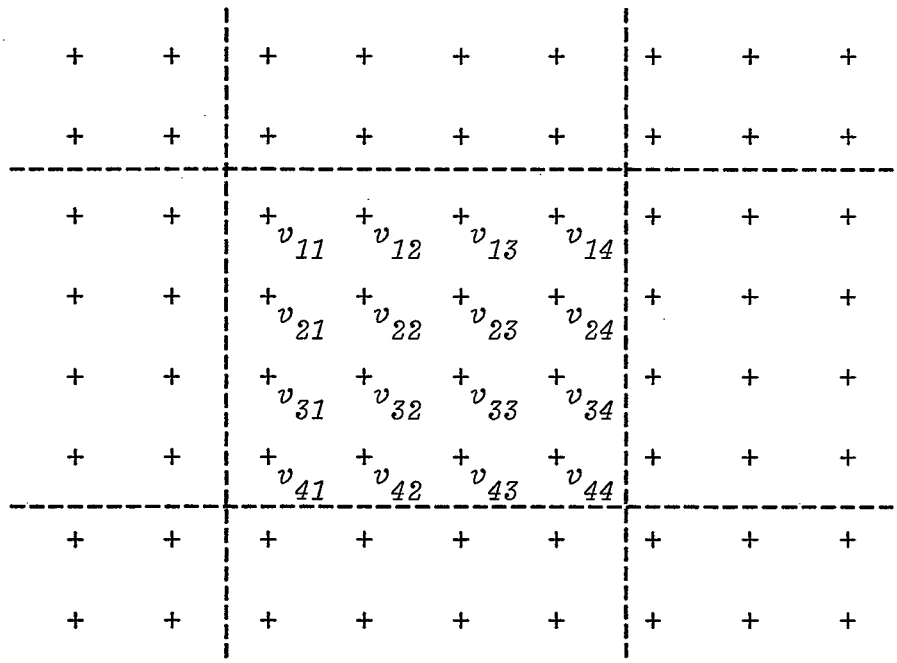

Quantizer input vector:

$$\mathbf{x} = (x_1, x_2, \ldots, x_k)$$
$$= (v_{11}, v_{12}, v_{13}, v_{14},$$
$$v_{21}, v_{22}, v_{23}, v_{24},$$
$$v_{31}, v_{32}, v_{33}, v_{34},$$
$$v_{41}, v_{42}, v_{43}, v_{44}),$$

where here k = 16.

Fig. 4.5 Quantizer input vector

(The symbol "+" denotes a picture element).

4.4.2 Quantizer Q^G and Q^H

Let Q^G and Q^H denote the quantizers which are optimized by using, as training sequences, GIRL and HOME, respectively. The codebook rate R = 8 [bits], and therefore the per-symbol codebook rate $\overline{R}$ = 0.5 [bits]. A block of picture elements, which consist a quantizer input vector, is compared with all of the 2^R = 256 reproduction vectors, and is approximated by the reproduction vector which provides the minimum distortion.

The signal-to-noise ratio is shown in Table 4.3.

Table 4.3 Results of simulations for Q^G and Q^H.

Sources	Quantizers	
	Q^G (GIRL)	Q^H (HOME)
GIRL	31.6 dB	27.6 dB
HOME	26.3 dB	29.3 dB

It is seen from the Table that the quantizer Q^G, which is optimized by using GIRL, provides good performance for GIRL, whereas it provides rather poor performance for HOME. The performance degradation is of 5.3 dB in signal-to-noise ratio. Figure 4.6 demonstrates the reproduced image data when the quantizer Q^G is applied to GIRL and HOME. It is seen from Fig. 4.6 (a) that Q^G provides good reproduction

(a) GIRL

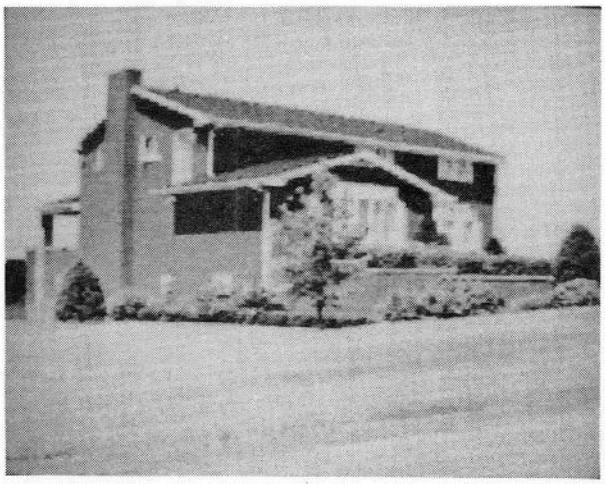

(b) HOME

Fig. 4.6 Images quantized by Q^G ($\overline{R}$ = 0.5 bits).

(a) GIRL

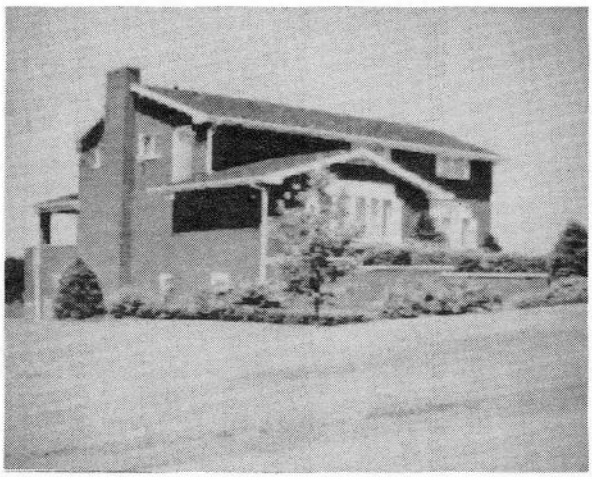

(b) HOME

Fig. 4.7 Images quantized by Q^H ($\overline{R}$ = 0.5 bits).

from the subjective standpoint as well as the objective standpoint. It is also seen from Fig. 4.6 (b) that the edges , where the abrupt change in gray levels exists, are not reproduced satisfactorily by Q^G. This can be explained in terms of the mismatch between the quantizer and the source as discussed in Chapter 3. In this case, HOME has fairly different statistical properties [30] from that of GIRL and the quantizer Q^G reflects the statistical characteristics of GIRL since it is GIRL that we used for optimizing the quantizer.

Similarly to the case above, the quantizer Q^H does not give good reproduction when it is applied to GIRL. The degradation is of 1.7 dB in signal-to-noise ratio and this seems to be acceptable as compared with that of Q^G. However, the degradation is fairly visible as shown in Fig. 4.7, where the quantizer Q^H is applied to GIRL and HOME.

4.4.3 Quantizer Q^+

The quantizer mismatch, as discussed above, can be improved by concatenating the reproduction alphabets of the quantizer Q^G and Q^H. This method, which will be referred to as the concatenation of reproduction alphabet, can be formulated as follows:

Consider the quantizers Q^1 and Q^2 which have the reproduction alphabets $\mathbf{Y}^1$ and $\mathbf{Y}^2$, where

$$\mathbf{Y}^1 = \{ \mathbf{y}_i^1 \; ; \; i=1,2,\ldots,N_1 \},$$

$$\mathbf{Y}^2 = \{ \mathbf{y}_i^2 \; ; \; i=1,2,\ldots,N_2 \}.$$

The concatenated reproduction alphabet $\mathbf{Y}^+$ can be constructed as

$$\begin{aligned}\mathbf{Y}^+ &= \mathbf{Y}^1 \cup \mathbf{Y}^2 \\ &= \{ \mathbf{y}_i^+ \; ; \; i=1,2,\ldots,N_+=N_1+N_2 \}.\end{aligned}$$

Let Q^+ denote the resultant quantizer which is defined by both the reproduction alphabet $\mathbf{Y}^+$ and the optimal partition which is derived from the concatenated reproduction alphabet $\mathbf{Y}^+$. The codebook rates of the quantizers Q^1, Q^2 and Q^+ are defined by

$$\begin{aligned}R_1 &= \log_2 N_1, \\ R_2 &= \log_2 N_2, \text{ and} \\ R_+ &= \log_2 N_+ = \log_2(N_1+N_2),\end{aligned}$$

respectively.

Table 4.4 shows that signal-to-noise ratio obtained by the quantizer Q^+. It is easily seen from the Table that the quantizer Q^+ provides good performance for both image data. Since $R_1 = R_2 = 8$ [bits], $R_+ = 9$ [bits]. Consequently, the per-symbol codebook rate of Q^+ is $9/16 \cong 0.56$ [bits] and thus the increase in per-symbol codebook rate over Q^G and Q^H is only $1/16 \cong 0.06$ [bits].

Table 4.4 Results of simulations for Q^+.

Sources	Quantizer
	Q^+ (Q^G + Q^H)
GIRL	31.9 dB
HOME	29.8 dB

(a) GIRL

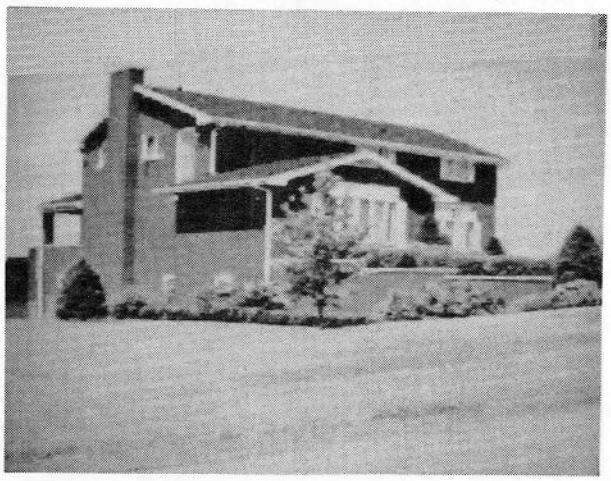

(b) HOME

Fig. 4.8 Images quantized by Q^+ ($\overline{R} \cong 0.56$ bits).

Figure 4.8 demonstrates the reproduced image when the quantizer Q^+ is applied to GIRL and HOME. It is seen from the Figure that the reproduction is fairly good for both image data.

4.5 conclusion

In this Chapter the vector quantization is applied to the video signals, and proved to provide good performance. It is found that the maximum error distortion measure can be used even if the MSE fidelity criterion is assumed.

A novel design method, the concatenation of reproduction alphabet, offers in improving the performance when the quantizer mismatch occurs.

It is demonstrated that the signal-to-noise ratio of approximately 30 dB can be achieved for both image data, GIRL and HOME, which have fairly different statistical characteristics.

Chapter 5

Conclusion

We have been investigated the performance of the vector quantization with the difference distortion measures. In this Chapter, we shall summarize the principal results revealed in this research.

In Chapter 1, the motivation of this work is given with the basic concept of the quantization.

In Chapter 2, we have derived the asymptotic bounds to the optimal performance of vector quantizers with finite block length, wherein the bounds are generalized to the difference distortion measures that are increasing functions of the seminorm of their argument. This provides a k-dimensional generalization of the Gish and Pierce's result for scalar quantizers and also a natural generalization of Gersho's result for the distortion measures that are powers of the Euclidean norm. When the distortion measure is a power of a seminorm the bounds are shown to be strictly better than the corresponding bounds provided by the k-th order rate distortion functions.

In Chapter 3, using the bound derived in Chapter 2, we have investigated the asymptotic performance of variance-mismatched vector quantizers and have demonstrated that well-designed vector quantizers are inherently more invulnerable to variance mismatch than conventional scalar quantizers. The results of simulations confirm this robustness of the vector quantizers.

In Chapter 4, we have applied the vector quantization to video signals. Based on the asymptotic analysis in Chapter 2, it has been shown that the vector quantization with maximum error distortion measure can be used for relaxing the computational complexity of the vector quantization even when the fidelity criterion is based on the mean-squared-error. Computer simulations demonstrate the effectiveness of the vector quantization for real video signals.

The mathematical structures of the reproduction alphabets and/or partitions have not been discussed throughout this work, since we focused the performance analysis of the vector quantizers. This research will proceed to investigate the structure of the vector quantizers for obtaining the fast quantizing algorithms, which allow us to implement the LSI chips performing the real-time vector quantization.

We complete the paper with hope that, in the near future, the LSI vector quantizers will act the leading role in the efficient video and speech data compression systems.

Appendix

Lemma: For $\alpha \geq 0$,

$$\Gamma(\alpha+1) \geq \left(\frac{\alpha + 1}{e}\right)^{\alpha} .$$

Proof:

Rewrite the inequality as

$$f(\alpha) = \log \Gamma(\alpha+1) - \alpha \log(\alpha+1) + \alpha \geq 0$$

and observe that it holds with equality at $\alpha = 0$. Next consider the derivative

$$f'(\alpha) = \frac{\Gamma'(\alpha+1)}{\Gamma(\alpha+1)} + \frac{1}{\alpha+1} - \log(\alpha+1) \quad . \qquad (A.1)$$

The function $\psi(\beta) = \Gamma'(\beta)/\Gamma(\beta)$ (called the "psi" or "digamma" fuction) satisfies [15,p.664]

$$\int_0^1 \psi(\beta+t)dt = \log \beta \quad , \quad \beta > 0.$$

In addition, $\psi(\beta)$ is nondecreasing in β and hence $\psi(\beta+1) \geq \log \beta$. We also have, however, that since $\Gamma(\beta+1) = \beta\Gamma(\beta)$ and $\Gamma'(\beta+1) = \beta\Gamma'(\beta) + \Gamma(\beta)$, then

$$\psi(\beta+1) = \frac{\Gamma'(\beta+1)}{\Gamma(\beta+1)} = \frac{\Gamma'(\beta)}{\Gamma(\beta)} + \frac{1}{\beta}$$

whence

$$\frac{\Gamma'(\beta)}{\Gamma(\beta)} \geq \log \beta - \frac{1}{\beta} .$$

Choosing $\beta = \alpha + 1$ we have from (A.1) that $f'(\alpha) \geq 0$ for $\alpha \geq 0$, and therefore $f(\alpha)$ must be increasing from 0 for $\alpha > 0$ which proves the lemma.

References

[1] Rosenfeld, A. and A. C. Kak, Digital image processing, New York, Academic Press, 1976.

[2] Cattermole, K. W., Principle of pulse code modulation, London, Iliffe Books, 1969.

[3] Tazaki, S. and Y. Yamada, "Vector quantization," J. IECE of Japan, vol. 67, pp.532-536, 1984.

[4] Berger, T., Rate Distortion Theory, Englewood Cliffs, NJ, Prentice-Hall, 1971.

[5] Yamada, Y., S. Tazaki, and R. M. Gray, "Asymptotic performance of block quantizers with difference distortion measures," IEEE Trans. Inform. Theory, vol. IT-26, pp.6-14, 1980.

[6] Tazaki, S., Y. Yamada, and R. M. Gray, "Evaluation of two-dimensional quantization,"Digital Signal Processing (Selected Papers from the International Conference on Digital Signal Processing, Firenze, Italy, 1978), edited by V. Cappelini and A. G. Constantinides, p.117-121, Academic Press, 1980.

[7] Yamada, Y. and S. Tazaki, "Efficient two-dimensional quantization of Laplacian source with magnitude-error criterion," Proceedings of First Symposium on Information Theory and its Applications, pp.33-37 1978.

[8] Gersho, A.,"Asymptotically optimum block quantization," IEEE Trans. Inform. Theory, vol.IT-25, no.4, pp.373-380,July, 1979.

[9] Bennet, W. R.,"Spectra of quantized signals,"Bell Syst. Tech. J., vol.27, pp.446-472, July, 1948.

[10] Gray, R. M. and A. H. Gray, Jr.,"Asymptotically optimal quantizers,"IEEE Trans. Inform. Theory, vol. IT-23, pp.143-144, Jan. 1977.

[11] Gish, H. and J. N. Pierce,"Asymptotically efficient quantizing," IEEE Trans. Inform. Theory, vol. IT-14, pp.676-683, Sept. 1968.

[12] Algazi, V. R., "Useful approximation to optimum quantization," IEEE Trans. Commun, Tech., vol.COM-14,pp.297-301, 1966.

[13] Yamada, Y. and S. Tazaki,"Generalized bound for multidimensional quantization," in 1978 Joint Conv. Rec. of the Societies Related with Electrical and Electronics Engr. at Shikoku District in Japan, pp.4-2, 1978.

[14] Gray, A. H., Jr., R. M. Gray and J. D. Markel,"Comparison of optimal quantizations of speech reflection coefficients," IEEE Trans. Acous., Speech, Signal Processing, vol. ASSP-25, pp.9-23, Feb. 1977.

[15] Gradshteyn, I. S. and I. M. Ryzhik, Table of Integrals Series and Products, New York, Academic Press, 1972.

[16] Rudin, W., Real and Complex Analysis, New York, McGraw-Hill, 1966.

[17] Ash, R., Real Analysis and Probability, New York, Academic Press, 1972.

[18] Lin'kov, Yu. N., "Evaluation of ε-entropy of random variables for small ε," Prob. Inform. Trans., vol.1, pp.12-18, 1965.

[19] Yamada, Y., S. Tazaki, M. Kasahara, and T. Namekawa, "Variance mismatch of vector quantizers," IEEE Trans. Inform. Theory, vol. IT-30, pp104-107, 1984.

[20] Yamada, Y., and S. Tazaki, "Asymptotic performance of mismatched block quantizers," Proceedings of Third Symposium on Information Theory and its Applications, pp.121-123, 1980.

[21] Gray, R. M. and L. D. Davisson, "Quantizer mismatch," IEEE Trans. Commun., vol. COM-23, pp.439-443, Apr.1975.

[22] Mauersberger, M., "Experimental results on the performance of mismatched quantizers," IEEE Trans. Inform. Theory, vol. IT-25, pp.381-386, July 1979.

[23] Miller, J. H. and J.B. Thomas, "Detectors for discrete-time signals in non-Gaussian noise," IEEE Trans. Inform. Theory, vol. IT-18, pp.241-250, Mar. 1972.

[24] Linde, Y., A. Buzo, and R. M. Gray, "An algorithm for vector quantizer design," IEEE Trans. Commun., vol.COM-28, pp.84-95, 1980.

[25] Yamada, Y. and S. Tazaki, "Vector quantizer design for video signals," IECE Trans., vol. J66-B, pp.965-972, 1983.

[26] Yamada, Y., K. Fujita, and S. Tazaki, "Vector quantization of video signals," Proceedings of Annual Conference of IECE of Japan, pp. 1031, 1981.

[27] Yamada, Y., K. Fujita, and S. Tazaki, "A consideration on the block quantization of the image," Technical Report of IECE, CS79-235, p.9-12, 1980.

[28] Netravali, A. N. and J. O. Limb, "Picture coding: a review," Proc. IEEE, vol. 68, pp.366-406, 1980.

[29] Paez, M. D. and T. H. Glisson ,"Minimum mean-squared-error quantization in speech PCM and DPCM systems," IEEE Trans. Commun., vol. COM-20, pp.225-230, 1979.

[30] Onoe, M., M. Sakauchi, and Y. Inamoto, "Standard image data base," MIPC Report 79-1, Multidimensional Image Processing Center, Institute of Industrial Science, University of Tokyo, 1979.